PONTIFÍCIA UNIVERSIDADE CATÓLICA DO RIO GRANDE DO SUL
FACULDADE DE ODONTOLOGIA
PROGRAMA DE PÓS-GRADUAÇÃO EM ODONTOLOGIA
MESTRADO EM ODONTOLOGIA
ÁREA DE CONCENTRAÇÃO EM ENDODONTIA

CAROLINE MARCA

VARIABILIDADE DAS ÁREAS TRANSVERSAIS DO CANAL E DA RAIZ DE PRÉ-MOLARES SUPERIORES COM TRÊS RAÍZES ATRAVÉS DA MICROTOMOGRAFIA COMPUTADORIZADA E DA TOMOGRAFIA DE FEIXE CÔNICO

Porto Alegre
2011

CAROLINE MARCA

VARIABILIDADE DAS ÁREAS TRANSVERSAIS DO CANAL E DA RAIZ DE PRÉ-MOLARES SUPERIORES COM TRÊS RAÍZES ATRAVÉS DA MICROTOMOGRAFIA COMPUTADORIZADA E DA TOMOGRAFIA DE FEIXE CÔNICO

Dissertação apresentada como parte dos requisitos obrigatórios para obtenção do título de Mestre em Endodontia pelo Programa de Pós-Graduação da Faculdade de Odontologia da Pontifícia Universidade Católica do Rio Grande do Sul.

Orientador: Prof. Dr. José Antonio Poli de Figueiredo

Porto Alegre

2011

CAROLINE MARCA

VARIABILIDADE DAS ÁREAS TRANSVERSAIS DO CANAL E DA RAIZ DE PRÉ-MOLARES SUPERIORES COM TRÊS RAÍZES ATRAVÉS DA MICROTOMOGRAFIA COMPUTADORIZADA E DA TOMOGRAFIA DE FEIXE CÔNICO

Dissertação apresentada como parte dos requisitos obrigatórios para obtenção do título de Mestre em Endodontia pelo Programa de Pós-Graduação da Faculdade de Odontologia da Pontifícia Universidade Católica do Rio Grande do Sul.

Aprovada em ____ de _____________ de 2011.

BANCA EXAMINADORA:

____

Profª. Drª. Maria Ivete Bolzan Rockenbach

____

Profª. Drª. Patrícia Maria Poli Kopper Móra

____

Prof.Dr. José Antonio Poli de Figueiredo

Porto Alegre

2011

Dados Internacionais de Catalogação na Publicação (CIP)

M313v Marca, Caroline

Variabilidade das áreas transversais do canal e da raiz de pré-molares superiores com três raízes através da microtomografia computadorizada e da tomografia de feixe cônico / Caroline Marca. – Porto Alegre, 2011.

71 f.

Diss. (Mestrado) – PUCRS. Faculdade de Odontologia. Programa de Pós-Graduação em Odontologia. Área de concentração: Endodontia.

Orientador: Prof. Dr. José Antonio Poli de Figueiredo.

1. Odontologia. 2. Endodontia. 3. Tomografia

Computadorizada. 4. Canal Radicular (Anatomia). I. Figueiredo,

Bibliotecária Responsável: Dênira Remedi – CRB 10/1779

Dedico esta dissertação aos meus pais, que sempre me incentivaram a acrescentar...

AGRADECIMENTOS

Agradeço a Deus por estar comigo, ao meu anjo da guarda, por me guiar.

É difícil agradecer as dificuldades, mas com elas se cresce...

Aos meus pais, Romeu e Irene, pela minha vida, pela minha formação pessoal e profissional, pelo incentivo nos estudos, por mostrar a direção, e nos momentos de fraqueza, pela força.

Ao meu marido, Rafael, meu amor, pelo seu amor, por tanta paciência e compreensão, e pela ajuda direta nesta dissertação.

Aos meus irmãos Fernando e Felipe, cunhadas Patrícia e Fabíola, sobrinhos Israel, Giovana e Laura, por serem parte da minha vida e pelo apoio.

Ao meu querido orientador, Prof. Dr. José Antonio Poli de Figueiredo, modelo inegável de contribuição na odontologia, exemplo de professor, pessoa e amigo, pela orientação e comprometimento neste trabalho, e confiança a mim depositada.

Aos meus queridos mestres e amigos, Prof. Dr. Marcus Vinícius Reis Só e Profª. Dra Fabiana Vieira Vier Pelisser, meus inspiradores, que sempre estimularam meu crescimento profissional, obrigada por nossa amizade e pela oportunidade de trabalharmos juntos. À profª. Dra. Fabiana Vieira Vier-Pelisser, pela ajuda significativa nesta dissertação e à sua família, que sempre me acolheu como se fizesse parte dela.

Aos professores Dr. Paul Dummer e Susan Bryant, e a Universidade de Cardiff, pela presteza e oportunidade de realizar este trabalho juntos.

Ao prof. Dr. Vinicius Dutra pela sua atenção e colaboração, e à profª. Dra. Vânia Fontanella, exemplo de dedicação ao ensino, com seu auxílio, sempre disponível.

Aos meus professores do curso de pós-graduação: Dr. José Antonio Poli de Figueiredo, Dra. Maria Martha Campos, Dra. Patrícia Poli, Dr. Eraldo Batista Junior, Dr. João Batista Weber, Dra. Fabiana Vieira Vier-Pelisser, Dra. Marília Gerhardt de Oliveira, Dr. Mario Wagner, pela dedicação e ensinamentos científico-intelectuais.

À secretaria da Pós-Graduação: Ana Prestes, Cláudia Reginato, Davenir Brusch, Marcos Correa e Paulo da Silva, pela disponibilidade e acolhimento.

Ao Ministério da Educação, através da Capes, pelo incentivo aos alunos do Programa de Pós-Graduação em Odontologia da PUCRS, no desenvolvimento da ciência brasileira e na formação de novos docentes e pesquisadores.

À PUCRS, pela oportunidade de realizar um curso tão qualificado.

À Clínica Rosa Odontologia, à Odontoclínica Wallau, à colega Fabíola Baldissera, pela parceria. Aos meus pacientes, que foram pacientes até na minha ausência.

Aos meus queridos colegas de curso, Alessandra Trindade, Andrea Fredrich, Carina Follmann, Carlos Wolle, Charles Pereira, Claudia Wagner, Deborah Cogo, Fernanda Lopes, Grasiela Grundling, Janaina Kufner, Kathrein Tapia, Larissa Klassmann, Lenara Dondoni, Marília Burgel, Matheus Souza, Pabla Sechi, Renata Morgental e Roberta Scarparo, que ao meu lado estiveram, pelas boas risadas, pelo ombro amigo e cumplicidade. A amizade foi o maior legado.

A todos que de uma maneira ou outra me ajudaram no Mestrado, muito obrigada.

RESUMO

Introdução: Este estudo analizou a variação das áreas transversais do canal e da raiz de pré-molares superiores com três raízes através da microtomografia computadorizada (µTC) e da tomografia de feixe cônico (TCFC). **Métodos:** Dezesseis pré-molares superiores, *ex vivo*, com três raízes distintas e ápices completamente formados foram escaneados usando a µTC e a TCFC. As áreas transversais das raízes e dos canais radiculares foram mensuradas, através do Photoshop CS: a mais cervical e a mais apical de cada terço radicular, em ambas as técnicas tomográficas, e 30 secções radiculares eqüidistantes, nas imagens de µTC. Áreas de raízes e de canais foram comparadas, para cada método, usando o teste t de Student para amostras emparelhadas, com intervalo de confiança de 95%. **Resultados:** As imagens da µTC apresentaram maior nitidez, em relação às TCFC. Houve diferença estatisticamente significante quando as médias de áreas de raízes e canais radiculares foram analisadas pela µTC e pela TCFC, na maioria dos terços radiculares ($p<0.05$). As áreas de raízes e de canais radiculares tiveram o mesmo tipo de variação para todas as raízes, diminuindo proporcionalmente de cervical para apical, até as imediações do início do canal cementário, onde a área aumentou em direção apical. **Conclusão:** Embora a variabilidade tenha sido a mesma, nas raízes e nos canais estudados, a TCFC em comparação à µTC, mostrou-se inferior em relação ao detalhamento de imagens.

Palavras chave: anatomia do canal radicular, pré-molar superior, microtomografia computadorizada, tomografia de feixe cônico.

ABSTRACT

Introduction: This study analyzed variations in canal and root cross-sectional area in three-rooted maxillary premolars between high-resolution computed tomography (µCT) and cone beam computed tomography (CBCT). **Methods:** Sixteen extracted maxillary premolars with three distinct roots and fully formed apices were scanned using µCT and CBCT. Photoshop CS software was used to measure root and canal cross-sectional areas at the most cervical and the most apical points of each root third in images obtained using the two tomographic computed (CT) techniques, and at 30 root sections equidistant from both root ends using µCT images. Canal and root areas were compared between each method using the Student *t* test for paired samples and 95% confidence intervals. **Results:** Images using µCT were sharper than those obtained using CBCT. There were statistically significant differences in mean area measurements of roots and canals between the µCT and CBCT techniques ($p<0.05$) Root and canal areas had similar variations in cross-sectional µCT images and became proportionally smaller in a cervical to apical direction as the cementodentinal junction was approached, from where the area then increased apically. **Conclusion:** Although variation was similar in the roots and canals under study, CBCT produced poorer image details than µCT.

Key words: root canal anatomy, maxillary premolar, high-resolution computed tomography, cone beam computed tomography.

SUMÁRIO

1 INTRODUÇÃO

O índice do insucesso endodôntico pode ser relacionado ao desconhecimento da anatomia interna e externa, ou a não localização, instrumentação e obturação de um determinado canal radicular. Os pré-molares superiores (PmS) apresentam uma complexidade anatômica devido a significativas ramificações do sistema de canais radiculares, que se acentua naqueles que apresentam três canais radiculares e/ou com bifurcação apical do canal radicular principal (1). A presença de PmS portadores de três raízes distintas tem baixa ocorrência e pode variar de 0,5% (2) a 6% (3).

Vários métodos vêm sendo empregados para o estudo da anatomia do canal radicular: clarificação (4 -13), desgaste (5, 6, 10, 13), exame radiográfico (11, 14, 15, 16) e, mais recentemente, a tomografia computadorizada (16 - 23).

A tomografia computadorizada (TC) é um método de diagnóstico que utiliza radiação X a qual reproduz, tridimensionalmente, em imagens, partes do corpo humano (24), revelando estruturas anatômicas e processos patológicos (24, 25).

A tomografia computadorizada de feixe cônico (TCFC) vem sendo empregada clinicamente na odontologia, pois proporciona uma baixa dose de radiação, tendo um tempo total de exame que varia de 10 a 70 segundos, e de 3 a 6 segundos de exposição à radiação (24).

A microtomografia computadorizada (µTC) é considerada um avanço das técnicas de inspeção por raios X, por ser um procedimento não invasivo e de alta precisão, embora necessite de alta radiação (25) e um tempo de exposição de 20 minutos até várias horas (26).

Os tomógrafos possuem uma fonte de raios X, um suporte e um detector de imagem (26). O diferencial da µTC está relacionado ao tamanho do foco do tubo de raios X. Quanto menor for o diâmetro do foco do tubo de raios X, melhor se dará a focalização das estruturas inspecionadas, qualificando a imagem adquirida (25).

A TCFC e a µTC apresentam muitas vantagens em comparação com as técnicas previamente usadas para avaliação da morfologia. As técnicas são totalmente conservadoras e não invasivas podendo ser empregadas no treinamento pré-clínico e no estudo de procedimentos endodônticos e restauradores. Análises em três dimensões podem ser feitas tanto qualitativamente, quanto quantitativamente. Anatomia interna e externa pode ser vistas juntas ou separadas (17, 23, 24, 25, 27).

As imagens bidimensionais digitais são formadas com referência na largura e na altura, pelos pixels. Como a imagem tomográfica é tridimensional, um novo plano é adicionado, a profundidade, então a unidade formadora será o voxel. O voxel é a menor unidade da imagem tomográfica e pode ter diferentes tamanhos, conforme a região do corpo a ser escaneada e a qualidade da imagem desejada. Quando se quer imagens precisas de pequenas áreas, ajusta-se o aparelho para adquirir cortes de menor espessura. Um corte de 1mm de espessura, terá um voxel de 1mm (24).

Na TCFC, o voxel apresenta medidas de altura, largura e profundidade iguais, sendo cada uma destas, menor que 1mm, normalmente de 0,119 a 0,4mm. Com isso a imagem de TCFC apresenta boa resolução (24). Um voxel de 0,3mm parece ter melhor desempenho, associado à baixa exposição à radiação X, quando comparado com o de 0,2 e 0,4 mm, na avaliação de reabsorção externa simulada (28).

A µTC tem sido validada na Endodontia experimental, devido particularmente ao aumento substancial da definição da imagem, uma vez que a distância entre os cortes passou de 1mm para 34µm (29). Conseqüentemente um elevado número de secções é gerado e fica disponível para observação, podendo ser considerada esta, outra grande vantagem (17). A µTC trouxe informações comparáveis às da histologia, servindo como padrão ouro para estudos *in vitro* (18).

A metodologia apresentada pioneiramente no estudo tridimensional do canal radicular, através da µTC, serviu como base para análise da anatomia do canal, na Endodontia experimental (30). Com a µTC avaliaram-se: o volume de instrumentação do canal (31, 32), a relação entre a macromorfologia interna e externa radicular (33), a curvatura dos canais radiculares (34), a prevalência de istmos (17), além do efeito de técnicas de instrumentação na forma dos canais radiculares (29, 30, 32, 35 - 38). A anatomia do sistema de canais radiculares de pré-molares trirradiculados avaliada através da µTC foi recentemente reportada (23).

Por meio da TCFC estudaram-se a influência do tamanho do voxel, na capacidade de diagnóstico de reabsorção radicular externa simulada (28), a identificação do sistema de canais radiculares (19, 22), a avaliação do comprimento e homogeneidade da obturação de canais (39) e a comparação de instrumentos empregados para o preparo cervical (40), entre outros.

A comparação entre a µTC e a TCFC, utilizando voxels de 41 e 76 µm, respectivamente, na mensuração de 120 germes dentários de 16 mandíbulas de crianças, mostrou que tais técnicas foram estatisticamente semelhantes (41).

Com base no exposto, evidenciou-se a ausência de estudos referentes à variação da área radicular e do canal de PmS com três raízes utilizando métodos mais precisos de observação, que mantivessem a integridade da estrutura dentária. Portanto a aplicabilidade da µTC e da TCFC, como instrumentos de análise detalhada da anatomia de PmS com três raízes, tornou-se oportuna.

2. ARTIGO

Submetido ao Journal of Endodontics - Fator de impacto: 2.953

Variations in cross-sectional area of three-rooted maxillary premolar roots and canals analyzed using high-resolution computed tomography and cone beam tomography

Caroline Marca[a] BDS; Paul M. H. Dummer[b] BDS, MScD, PhD, DDSc, FDS RCS; Susan Bryant[b] BDS; Fabiana Viera Vier-Pelisser[a] BDS, MSc, PhD; Marcus Vinicius Reis Só[c] BDS, MSc, PhD; Vania Fontanella[d] BDS, MSc, PhD; Vinicius D'avila Dutra[e] BDS, PhD; José Antonio Poli de Figueiredo[a] BDS, MSc, PhD.

[a] Department of Endodontics, Graduate Program, School of Dentistry, Pontifical Catholic University of Rio Grande do Sul (PUCRS), Porto Alegre, Brazil;

[b] School of Dentistry, Cardiff University, Cardiff, UK;

[c] Department of Endodontics, Graduate Program, School of Dentistry, Federal University of Rio Grande do Sul (UFRGS), Porto Alegre, Brazil;

[d] Department of Oral Radiology, Graduate Program, School of Dentistry, Brazilian Lutheran University (ULBRA), Canoas, RS, Brazil;

[e] CDI - Imaging Diagnosis Centre, Porto Alegre, Brazil.

Address correspondence to:

José Antônio Poli de Figueiredo
Graduate Program in Dentistry
Pontifical Catholic University of Rio Grande do Sul – PUCRS, Porto Alegre, Brazil
Corresponding address:
Av. Ipiranga 6681 Prédio 6 sala 206
CEP 90619-900 Porto Alegre – RS – Brazil
Phone: 55 51 3320 3500 ext. 4307

Variations in cross-sectional area of three-rooted maxillary premolar roots and canals analyzed using high-resolution computed tomography and cone beam tomography

ABSTRACT

Introduction: This study analyzed variations in canal and root cross-sectional area in three-rooted maxillary premolars between high-resolution computed tomography (µCT) and cone beam computed tomography (CBCT). **Methods:** Sixteen extracted maxillary premolars with three distinct roots and fully formed apices were scanned using µCT and CBCT. Photoshop CS software was used to measure root and canal cross-sectional areas at the most cervical and the most apical points of each root third in images obtained using the two tomographic computed (CT) techniques, and at 30 root sections equidistant from both root ends using µCT images. Canal and root areas were compared between each method using the Student *t* test for paired samples and 95% confidence intervals. **Results:** Images using µCT were sharper than those obtained using CBCT. There were statistically significant differences in mean area measurements of roots and canals between the µCT and CBCT techniques ($p<0.05$) Root and canal areas had similar variations in cross-sectional µCT images and became proportionally smaller in a cervical to apical direction as the cementodentinal junction was approached, from where the area then increased apically. **Conclusion:** Although variation was similar in the roots and canals under study, CBCT produced poorer image details than µCT.

Key words: root canal anatomy, maxillary premolar, high-resolution computed tomography, cone beam computed tomography.

Introduction

High-resolution computed tomography (µCT) systems reproduce accurately the structures of small specimens in three-dimensional images (1). Although an advance over conventional CT because of its higher resolution µCT emits high doses of radiation (2) and is not available for clinical use. The cone beam computed tomography (CBCT), can be used on patients as it exposes them to a lower radiation dose (3). Both techniques have advantages over those used previously to evaluate tooth morphology largely because they are not invasive (, 3).

Several studies have used µCT, such as three-dimensional evaluation of root canals (4), volume of the instrumented canal (1, 5), association between internal and external root macromorphology (6), root canal curvature (7), prevalence of isthmuses (8), as well as instrumentation techniques (4, 5, 9, 10, 11,). CBCT has been used in studies evaluating the effect of voxel size when assessing simulated external root resorption (12), identification of the root canal system (13), length and homogeneity of root fillings (14) and comparison of cervical canal preparation instruments (15). A study comparing these techniques showed similar results when tooth germs were subjected to volume measurements (16).

A recent study described the anatomy of the root canal system in three-rooted maxillary premolars evaluated using µCT (17). However, no studies have evaluated variation in root area within three-rooted maxillary premolars using such accurate assessment methods maintaining the integrity of tooth structure. Therefore, this study evaluated the applicability of µCT and CBCT as techniques to study the anatomy of three-rooted maxillary premolars.

Material and Methods

The study was approved by the Ethics in Research Committee of Pontifícia Universidade Católica do Rio Grande do Sul (PUCRS - protocol no. 10/05068).

Sample selection

The sample comprised 16 three-rooted human maxillary premolars with fully formed apices that had been extracted for therapeutic reasons. Teeth were excluded if they had restorations or caries that reached the pulp chamber or the root. Teeth were stored individually in 0.1% thymol (Bellafarma, Caxias do Sul, Brazil).

High-resolution computed tomography

For the µCT analysis, the teeth were individually scanned cross-sectionally using a high-resolution desk-top µCT system at 50 kV (Skyscan 1072 Kontich, Belgium) in the School of Dentistry, Cardiff University (Cardiff, Wales, United Kingdom). For each tooth, 405 to 500 slices were obtained at a voxel size of 34 x 34 x 42 µm.

Cone beam computed tomography

Teeth were aligned with their crown facing up and root apex fixed to a utility wax base (Wilson, Polidental, Cotia, Brazil). The specimens were then scanned using an i-CAT CBCT scanner at 120 KVp (Imaging Sciences International, Inc, Hatfield, PA) in a radiological clinic (Dental Imaging Diagnosis Centre,Porto Alegre, Brazil). In all 90 to 118 sections per tooth were produced at a voxel size of 0.2 x 0.2 x 0.2 mm.

Measurement of the root and canal area

The images captured using the Skyscan and i-CAT software were converted into a bpm format. They were evaluated by one pre-calibrated examiner who measured the cross-sectional areas corresponding to the roots and the canals in selected sections of the root thirds. When the root had more than one canal, both were measured and their areas were added. When the roots were fused, the areas were measured according to the projection of each root.

Comparison between CT techniques

To compare CT techniques, the roots corresponding to the mesiobuccal (MB), distobuccal (DB) and palatal (P) canals were divided into cervical, middle and apical thirds (Fig. 1*A*). The reference points were the most cervical and most apical images of each root that had a canal lumen outlined by dentin. Two images of each third were selected for the measurement of each root and canal: the most apical and the most cervical.

Area variation

To study the variation in root and canal area in three-rooted maxillary premolars, only µCT images were used (Fig. 1*B*). In all 30 sections (10 equidistant sections in each root third: cervical, middle and apical) of each root (P, MB and DB) were evaluated.

Root and canal areas were measured using the Adobe Photoshop CS software (Adobe Systems Inc., San Jose, CA) according to the number of pixels; values were recorded in a Microsoft Excel 2003 spreadsheet (Microsoft Corporation, Redmond, WA). One image from each technique was transferred to the working area of AutoCAD software (Autodesk, San Rafael, CA). After the µCT and CBCT image scales were made equivalent, the root and canal perimeters were outlined and the areas were measured in mm^2. Calculations were made in triplicate, and the final area value was the mean of the three measurements. The values were then transformed from pixels to mm^2.

Statistical analysis of results

Mean and standard deviations were calculated for each root and canal third. The canal and root areas were compared for each method using the Student *t* test for paired samples and 95% confidence intervals. The level of significance was set at α=0.05. To evaluate area variation, mean root and canal areas were plotted in relation to each cross-section of the specimen on the µCT images. Data were analyzed using SPSS 18.0 (IBM, Armonk, NY) and SigmaPlot Graphics 11 (Systat Software, San Jose, CA).

Results

A total of 4032 root and canal area measurements were made using 3456 µCT and 576 CBCT images. The µCT images were sharper than the CBCT ones (Fig. 2*A*-*D*) and revealed a wealth of anatomic details, such as the presence of three and two canals in a MB and DB root in the middle third of one of the specimens (Fig. 2*A*), the presence of lateral canals (Fig. 2*B*), canal trifurcation in the apical third (Fig. 2*C* and *D*), as well as different shapes of root and canal sections. In contrast, the CBCT images were blurred (Fig. 2*E*-*H*).

Comparison between CT techniques

Table 1 shows that the root length measured using CBCT was shorter than when µCT was used.

Table 2 shows that there is a statistically significant difference ($p<0.05$) in most comparisons of root and canal area means between CT techniques in the different root thirds under study. When the root area was evaluated, areas measured using µCT tended to be greater than when CBCT was used to measure the cervical and middle thirds of all the roots. In the apical third, however, µCT measures were smaller.

When the canal area was evaluated, CBCT images had statistically greater areas than µCT in all the thirds of all the roots, except in the cervical thirds of the P and MB roots.

Area variation

Figure 3 describes absolute (root area + canal area) (*A*) and relative (canal area/root area + canal area) (*C*) variations. In general, variations were proportional in the different roots and thirds.

Absolute variation in MB and DB roots was similar, and the area decreased from cervical to apical. DB and P roots had the smallest and largest area values, respectively. In addition, P roots had a more marked variation than the other roots (Fig. 3*A*).

The analysis of canal area revealed that there was a decrease from cervical to apical up to a point close to the cementodentinal junction, where the area then increased apically, corresponding to the canal beyond the minor foramen (Fig. 3*B* and *C*).

Discussion

Maxillary premolars may have three roots (18). When they are not detected clinically or using conventional radiographic techniques, CBCT may be an important complementary diagnostic resource (13). Although it produces better image quality and detection of anatomic details, µCT is not used clinically because the scanner cannot be used for large samples and requires a long exposure time (2).

Results showed that the CT techniques were significantly different when used in the different root thirds (Table 2) and cannot, therefore, be compared. These differences may be explained by the lack of sharpness of the CBCT images (Fig. 2*E*-*H*) when compared with µCT images (Fig. 2*A*-*D*), which makes area measurements difficult, particularly for root canals, and also explaining the differences in the root lengths between the techniques (Table 1). CBCT images are blurred in comparison with µCT images due to scattering, a physical process in which radiation deflects from its straight trajectory in the medium through which it travels and is dispersed. This effect is uncommon in µCT, and the fact that it accurately describes anatomic details, such as the presence of more than one canal in each root, of lateral canals, apical deltas and variations of the cross-sectional area of the canal along its axis (17), makes it comparable to *in vitro* histology (19).

Human error when outlining the root and canal perimeters for area measurements might lead to incorrect measures. To avoid such a problem in this study, the Adobe Photoshop CS software was used for outlining and for the measurement of the root areas. This has shown to be useful in previous studies (16, 20).

CBCT and µCT were similar statistically in a study on volume reconstruction in tooth germs using voxel sizes that were closer to each other, 41 µm for µCT and 76 µm for CBCT (16). The present study followed parameters used in dental radiology, that is, 34 µm and 200 µm, and the ratio between methods was 3 times greater. Variations in voxel size may explain the differences in results from these studies, which may indicate that parameters currently used should be reconsidered. .

MB root and canal had a greater area than DB root in all the root thirds (Fig. 3*A*), perhaps because the buccopalatal distance of the MB root was greater than that of the DB root, particularly in the cervical and middle thirds (17). Maxillary first molars commonly contain two canals in the MB root (21). A relevant anatomic finding was the presence of 3 and 2 canals in the MB and DB roots in one specimen, which was demonstrated using µCT (Fig. 2*A*). Another study using µCT did not find 2 canals in the MB root in any of the specimens, but especially in the cervical third, the MB canal had a “comma-like” cross-section, with the isthmus positioned palatally (17), which was also found in other specimens in this study.

The curve of relative area variation, in all canals, increased starting from the 28th section. The mean distance between this and the last section was 0.50 mm for all the canals of the three-rooted maxillary premolar, or 0.61, 0.47 and 0.43 mm for the P, MB and DB canals. Other authors found a mean distance of 0.53 mm between the apical foramen and the constriction (22). Therefore, the significant increase of the canal area apically (Fig. 3*B* and *C*) may be explained by the presence of the cemental canal between the minor and major foramina.

References

1. Rhodes JS, Pitt Ford TR, Lynch JA, Liepins PJ, Curtis RV. Micro-computed tomography: a new tool for experimental endodontology. Int Endod J. 1999 May; 32(2): 165-70.

2. Robinson S, Suomalainen A, Kortesniemi M. µTC. Eur J Radiol. 2005 Nov; 56(2): 185-91.

3. Garib DG, Raymundo Jr. R, Raymundo MV, Raymundo DV, Ferreira SN. Tomografia computadorizada de feixe cônico (Cone beam): entendendo este novo método de diagnóstico por imagem com promissora aplicabilidade na Ortodontia. R Dental Press Ortodon Ortop Facial. 2007 Mar-Abr 2007; 12(2): 139-56.

4. Liedke GS, Silveira HED da, Silveira HLD da, Dutra V, Figueiredo JAP de. Influence of voxel size in the diagnostic ability of cone beam tomography to evaluate simulated external root resorption. J Endod. 2009 Fev; 35(2): 233-5.

5. Peters OA, Laib A, Rüegsegger P, Barbakow F. Three-dimensional analysis of root canal geometry by high-resolution computed tomography. J Dent Res. 2000 Jun; 79(6): 1405-9.

6. Peters OA, Peters CI, Schönenberger K, Barbakow F. ProTaper rotary root canal preparation: effects of canal anatomy on final shape analysed by micro CT. Int Endod J. 2003 Feb; 36(2): 86-92.

7. Bjorndal L, Carlsen O, Thuesen G, Darvann T, Kreiborg S. External and internal macromorphology in 3D-reconstructed maxillary molars using computerized X-ray microtomography. Int Endod J. 1999 Jan; 32(1): 3-9.

8. Lee JK, Ha BH, Choi JH, Heo SM, Perinpanayagam H. Quantitative three-dimensional analysis of root canal curvature in maxillary first molars using micro-computed tomography. J Endod. 2006 Oct; 32(10): 941-5.

9. Mannocci F, Peru M, Sherriff M, Cook R, Pitt Ford TR. The isthmuses of the mesial root of mandibular molars: a micro-computed tomographic study. Int Endod J. 2005 Aug; 38(8): 558-63.

10. Peters OA, Laib A, Göhring TN, Barbakow F. Changes in root canal geometry after preparation assessed by high-resolution computed tomography. J Endod. 2001 Jan; 27(1): 1-6.

11. Peters OA, Schönenberger K, Laib A. Effects of four Ni-Ti preparation techniques on root canal geometry assessed by micro computed tomography. Int Endod J. 2001 Apr; 34(3): 221-30.

12. Gambill JM, Alder M, Del Rio CE. Comparison Of nickel-titanium and stainless hand-file instrumentation using computed tomography. J Endod. 1996 Jul; 22(7): 369-75.

13. Matherne RP, Angelopoulos C, Kulild JC, Tira D. Use of cone-beam computed tomography to identify root canal systems in vitro. J Endod. 2008 Jan; 34(1): 87-9.

14. Sogur E, Baksi BG, Gröndahl HG. Imaging of root canal fillings: a comparison of subjective image quality between limited cone-beam CT, storage phosphor and film radiography. Int Endod J. 2007 Mar. 40(3): 179-85.

15. Sanfelice CM, Costa FB, Só MVR, Vier-Pelisser F, Bier CAS, Grecca FS. Effects of Four Instruments on Coronal Pre-enlargement by Using Cone Beam Computed Tomography. J Endod. 2010 May; 36(5): 858-61.

16. Maret D, Molinier F, Braga J, Peters AO, Telmon N, Treil J, Inglèse JM, Cossié A, Kahn JL, Sixou M. Accuracy of 3D reconstructions based on cone beam computed tomography. J Dent Res. 2010 Dec; 89(12): 1465-69.

17. Vier-Pelisser FV, Dummer PMH, Bryant S, Marca C, Só MVR, Figueiredo JAP. The anatomy of the root canal system of three-rooted maxillary premolars analysed using high-resolution computed tomography. Int Endod J. 2010 Dec; 43(12): 1122-31.

18. Kerekes K, Tronstad L. Morphometric observations on root canals of human premolars. J Endod. 1977 Feb; 3(2): 74-9.

19. Eder A, Kantor M, Nell A, Moser T, Gahleitner A, Schedle A, Sperr W. Root canal system in the mesiobuccal root of the maxillary first molar: an in vitro comparison study of computed tomography and histology. Dent maxillo fac radiol. 2006 May; 35(3): 175-7.

20. Vanzin ACM, Barletta FB, Fontanella V. Comparative assessment of root canal preparation by undergraduate students using manual and automated devices. Rev odonto ciênc. 2010 Jan-Mar; 25(1):69-73.

21. Barton DJ, Clark SJ, Eleazer PD, Scheetz JP, Farman AG. Tuned-aperture computed tomography versus parallax analog and digital radiographic images in detecting second mesiobuccal canals in maxillary first molars. Oral Surg Oral Med Oral Pathol Oral Radiol Endod. 2003 Aug; 96(2): 223-8.

22. Dummer PMH, Mc Ginn J, Rees DG. The position and topography of the apical canal constriction and apical foramen. Int Endod J. 1984 Oct; 17(4): 192-198.

LIST OF FIGURES

Figure 1. (*A*) Sites measured to compare µCT x CBCT techniques; red lines represent the most cervical and most apical sections of each root third; (*B*) 30 equidistant points (blue lines) were analyzed using µCT to study area variation.

Figure 2. Cross-section of maxillary premolar roots. Multiple canals (small arrows) in µCT images (*A*-*D*) and lack of details in CBCT images (*E*-*H*). Images in the same column correspond to neighbouring sections of the same tooth.

Figure 3. Absolute (*A*) and relative (*C*) variations of the cross-sectional areas in the different thirds: cervical (C), middle (M) and apical (A) from the µCT images. The figure in (*B*) represents the study findings in a diagrammatic representation to allow visualization of what was viewed in each root.

LIST OF TABLES

Table 1. Means and standard deviations of root lengths analyzed using µCT and CBCT

		CT technique	
Root	Third	µCT (mm)	CBCT (mm)
P	C	3.64 ± 0.6	2.81 ± 0.5
	M	3.60 ± 0.6	2.69 ± 0.4
	A	3.61 ± 0.6	2.71 ± 0.5
	C+M+A	10.84 ± 1.8	8.21 ± 1.4
MB	C	2.84 ± 0.6	1.85 ± 0.5
	M	2.81 ± 0.6	1.73 ± 0.5
	A	2.82 ± 0.6	1.79 ± 0.5
	C+M+A	8.46 ± 1.8	5.36 ± 1.6
DB	C	2.55 ± 0.6	1.58 ± 0.4
	M	2.53 ± 0.6	1.44 ± 0.4
	A	2.53 ± 0.6	1.50 ± 0.4
	C+M+A	7.61 ± 1.8	4.51 ± 1.2

P=palatal, MB=mesiobuccal, DB= distobuccal, C=cervical, M=middle, A=apical

Table 2. Means and standard deviations of root and canal cross-sectional areas in the different thirds using both CT techniques

		Root area			Canal area		
		CT technique			CT technique		
Root	Third	µCT (mm^2)	CBCT (mm^2)	P	µCT (mm^2)	CBCT (mm^2)	P
P	C	13.34 ± 2.8	11.26 ± 2.4	< 0.001	0.95 ± 0.4	0.90 ± 0.3	0.360
	M	9.42 ± 2.2	8.25 ± 1.8	< 0.001	0.39 ± 0.2	0.54 ± 0.2	0.002
	A	4.68 ± 1.2	5.29 ± 1.3	0.004	0.17 ± 0.7	0.30 ± 0.1	< 0.001
MB	C	7.54 ± 1.8	6.15 ± 1.3	< 0.001	0.31 ± 0.2	0.38 ± 0.2	0.031
	M	5.22 ± 1.2	4.82 ± 1.0	0.006	0.14 ± 0.07	0.27 ± 0.1	< 0.001
	A	2.61 ± 0.8	3.56 ± 0.9	< 0.001	0.06 ± 0.03	0.18 ± 0.09	< 0.001
DB	C	6.69 ± 1.8	5.48 ± 1.3	< 0.001	0.22 ± 0.1	0.32 ± 0.2	< 0.001
	M	4.71 ± 1.4	4.38 ± 1.0	0.163	0.13 ± 0.07	0.24 ± 0.1	< 0.001
	A	2.43 ± 1.0	3.27 ± 0.8	0.003	0.06 ± 0.03	0.17 ± 0.1	< 0.001

P=palatal, MB=mesiobuccal, DB= distobuccal, C=cervical, M=middle, A=apical

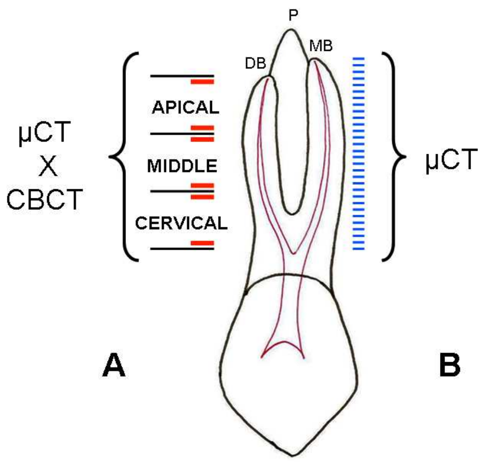

Figure 1

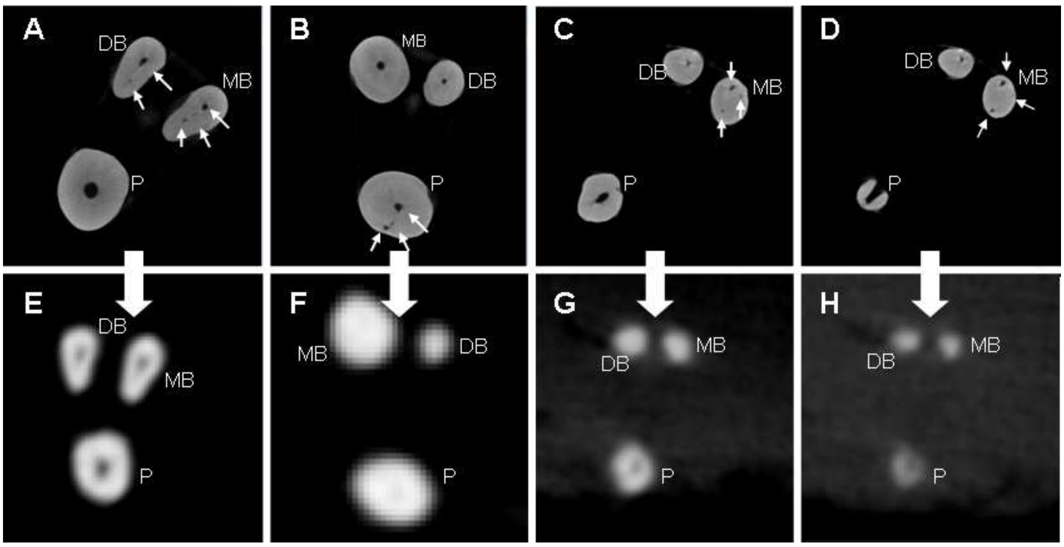

Figure 2

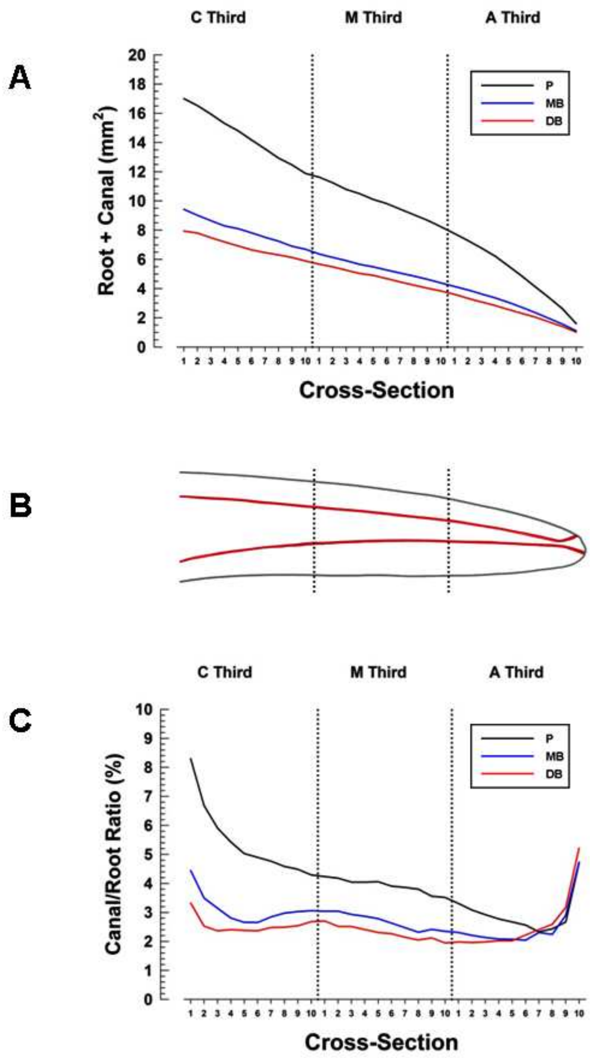
A
B
C
C Third
M Third
A Third
Root + Canal (mm2)
Canal/Root Ratio (%)
Cross-Section
P
MB
DB

Figure 3

3. DISCUSSÃO

O pré-molar superior (PmS) merece atenção especial devido à sua complexidade anatômica e a possibilidade de apresentar-se com 3 raízes distintas. A radiografia periapical muitas vezes pode ser limitada no reconhecimento dessas diversidades anatômicas, devido à sobreposição de estruturas (26). Caso isso não seja percebido radiograficamente e/ou clinicamente, a tomografia de feixe cônico (TCFC) será um recurso auxiliar de diagnóstico importante e justificável (19). A microtomografia (µTC), superior na qualidade de definição da imagem, com alto poder de resolução, proporciona um elevado número de secções disponíveis para observação, (17), e apresenta mais detalhes anatômicos (Fig. 2), embora esta não seja clinicamente praticável, pois o aparelho permite exclusivamente a inclusão de amostras pequenas, além de demandar tempo elevado e apresentar elevada radiação (26).

Este estudo teve como objetivo comparar a variação das áreas de raízes e de canais de pré-molares superiores trirradiculados, usando técnicas não invasivas de avaliação da morfologia, a µTC e a TCFC.

A µTC e a TCFC permitem, através de softwares próprios de cada técnica, a reconstrução tridimensional dos dentes, assim como a análise da morfologia em diferentes planos, mas para tal estudo, exclusivamente as secções transversais foram utilizadas. Diante do grande número de secções geradas, foram selecionados determinados pontos, com distâncias equivalentes, para posteriores mensurações, não comprometendo o estudo estatisticamente.

As técnicas tomográficas produziram imagens com qualidades bastante diferentes entre si (Fig. 2), com falta de nitidez das imagens de TCFC, em relação à µTC. Quanto menores e mais próximas forem suas secções, melhor será a resolução da imagem (42). Nas imagens microtomográficas foi possível observar detalhes anatômicos, como a presença de mais de um canal por raiz, de canais laterais, delta apical, variabilidade da secção transversal do canal ao longo do seu eixo (Fig. 2), assim como visto em outro estudo (23). As imagens de TCFC, não apresentaram tais detalhes, pois foram mais esfumaçadas em relação às de µTC. Nestas, a ocorrência de Scattering foi mais intenso, processo físico onde algumas formas de radiação são obrigadas a desviar-se de uma trajetória reta do meio através do qual passam, promovendo dispersão. Estas diferenças dificultam a mensuração da área, principalmente do canal (Tabela 2). Os resultados mostram que a µTC e a TCFC foram consideradas estatisticamente diferentes em muitos terços radiculares das raízes e dos canais (Tabela 2), não podendo ser comparadas, portanto.

Contrariamente ao presente estudo, a µTC e a TCFC foram consideradas semelhantes estatisticamente, na análise da reconstrução volumétrica de germes dentários (41). Tal pesquisa além de empregar metodologias diferentes, utilizou tamanhos de voxels mais próximos entre si, sendo de 41 e 76 µm, para a µTC e a TCFC, respectivamente, gerando, portanto, imagens mais semelhantes. No presente estudo empregou-se voxels de 34 µm e 200 µm, com uma relação entre os voxels deste e do outro trabalho, aproximadamente 3 vezes maior, explicando assim, o ocorrido.

Como as técnicas tomográficas se mostraram diferentes (Tabela 2), e com a µTC a observância de detalhes anatômicos foi notavelmente maior, além de ter melhor qualidade de imagens (Fig. 2), apenas as secções desta técnica foram utilizadas no estudo da variabilidade de áreas de canal e raiz, dos PmS trirradiculados. Esta metodologia foi consagrada como padrão-ouro para o estudo anatômico do sistema de canais radiculares, sendo comparada comparável à histologia, em estudos *in vitro* (18).

A mensuração das áreas poderia ter sido feita com o auxílio do programa AutoCAD, amplamente utilizado na arquitetura e engenharia, instrumento em diversas pesquisas da área da saúde e considerado um método de medida de alta precisão, além de ser de fácil para a quantificação de fenômenos biológicos (43). Mas para isso seria necessário delimitar, manualmente, os perímetros das raízes e dos canais, para o posterior cálculo das áreas, estando mais sujeitos à falha humana, o que poderia levar a medidas incorretas. Para que isso não ocorresse, este estudo valeu-se do programa Adobe Photoshop CS, também utilizado na quantificação de áreas radiculares (40, 44), que utiliza ferramentas de seleção de áreas, próprias do programa, tornando este método mais rápido e fidedigno. Em contrapartida, com o programa Adobe Photoshop CS, não se obteve valores aceitáveis na conversão de suas mensurações, que estavam em pixels, para mm^2. Então o AutoCAD foi aproveitado exclusivamente para proporcionar essa conversão, dos valores de área, de pixels para mm^2. Para isto, uma imagem da cada técnica foi transferida para a área de trabalho do AutoCAD. Para efeitos de equivalências de escalas, para a imagem da µTC empregou-se o valor 1 (igual ao da figura original) e para a imagem da CBCT, igual a 160, considerando o ângulo de rotação igual a zero. Os perímetros correspondentes à raiz e ao canal foram delimitados e as áreas, mensuradas, em mm^2. As mesmas imagens das duas técnicas tomográficas foram mensuradas no Photoshop em pixels. Assim, empregando uma regra de três simples, com a equivalência entre mesmas áreas mensuradas pelos dois programas, se fez a conversão dos valores em pixels e mm^2.

Antes da mensuração de áreas, houve uma preocupação quanto aos comprimentos das raízes avaliadas, já que a bi e/ou trifurcação poderiam ocorrer em terço apical, mas a amostra analisada se mostrou parelha (Tabela 1), embora com menores comprimentos encontrados na TCFC, devido à dificuldade na delimitação da área do canal em apical. Vale lembrar que não foi motivo do nosso trabalho contemplar a análise da altura de câmara pulpar, tampouco a localização da bi e trifurcação das raízes e dos canais, mas diante de PmS trirradiculados, sempre é importante lembrar do cuidado na abertura coronária, para não haja danos no assoalho da câmara pulpar, comprometendo a localização da entrada dos canais radiculares.

A variação de áreas dos PmS trirradiculares seguiu as configurações já descritas, onde a raiz palatina (P) é mais volumosa e cônica e a mésio-vestibular (MV) mais volumosa do que a disto-vestibular (DV) (Fig. 3*A*) (45). O conhecimento da estreita área do canal, no terço apical, principalmente nos canais MV e DV (Tabela 2), e da fragilidade radicular apical, alerta o clínico quanto à dificuldade de exploração desses canais, assim como a necessidade de cuidado durante o preparo das raízes vestibulares, que por serem mais finas, podem originar perfuração das suas paredes laterais, se uma instrumentação exagerada for conduzida (15). O menor diâmetro do canal, no último milímetro do ápice radicular de PmS trirradiculados, encontrado por outros autores, foi de 0.20mm (6). No presente estudo, o menor diâmetro de canal encontrado nas secções apicais foi de 0.28mm para os canais MV e DV, e 0.35mm para o canal P. A relevância clínica para este achado é notável, pois o tamanho do calibre do instrumento empregado no preparo do terço apical destes dentes deve contemplar todas as paredes do canal, sendo superior a um instrumento de número 30 para os canais, MV e DV, e 35 para o P, respectivamente.

A raiz e o canal MV apresentaram maior área do que a raiz e o canal DV, em todos os terços radiculares, provavelmente devido à maior distância vestíbulo-palatina da raiz MV em relação à DV, principalmente nos terços cervical e médio (23). Em função de similaridades anatômicas como a disposição das raízes no arco dental, o PmS trirradiculado é frequentemente chamado de mini-molar (14). Um achado comum com o 1º molar superior pode ser a presença de dois canais na raiz MV (46). Assim como demonstrado, em achados anatômicos relevantes do nosso estudo, a presença de 3 e 2 canais nas raízes MV e DV, respectivamente, em um único espécime, evidenciado na µCT (Fig. 2*A*). Adversamente, em outro estudo também empregando a µTC, neste mesmo elemento dental, a presença de 2 canais na raiz MV não foi notada em nenhuma das espécies (23). O canal MV, principalmente no terço cervical, teve sua secção em forma de vírgula, com istmos na direção palatina (23), fato este também comprovado em várias amostras deste estudo. Nestes casos, a utilização de soluções irrigadoras ou tecnologias (ultra-som, laser), que consiga abranger áreas onde o instrumento não atinge, como zonas de istmos, ramificações e deltas apicais, é de grande importância para o sucesso.

Neste estudo observou-se que a curva da variação da área relativa, em todos os canais, ascendeu aproximadamente a partir do 28º corte analisado (Fig. 3*C*). A distância média entre este e o último corte foi de 0.61, 0.47 e 0.43mm, para os canais P, MV, DV respectivamente, ou de 0.50mm para todos os canais. Uma distância média de 0.53mm, entre a constrição e o forame apical em PmS, foi encontrada por outros autores (47). O aumento significativo das áreas dos canais, em apical, pode ser justificado pela presença do canal cementário (Fig. 3*B* and *C*), com baixa influência da ocorrência de deltas apicais (Fig. 2*C* and *D*) em determinadas raízes, que também foram incluídos nas mensurações. Em poucos casos a saída foraminal se deu no vértice radiográfico confirmando outros achados (23).

O detalhamento das imagens trazido por estas técnicas tomográficas poderia ser explorado para a observação de mais aspectos, como a distância entre o vértice radiográfico e o forame apical dos PmS, assim como a quantificação de área, antes e depois da instrumentação, principalmente na porção apical. O uso da µTC e da TCFC, associado à histologia, em estudos *in vitro,* pode ser um campo a ser explorado na pesquisa endodôntica, para o estudo da anatomia destes e de outros elementos dentários.

4. REFERÊNCIAS

1. Lombart B, Michonneau JC. Anatomie des prémolaires et traitements endodontiques. Rev Belge Med Dent. 2005; 60(4): 322-36.

2. Pineda F, Kuttler Y. Mesiodistal and buccolingual roentgenographic investigation of 7,275 root canals. Oral Surg Oral Med Oral Pathol. 1972 Jan; 33(1): 101-10.

3. Carns EJ, Skidmore AE. Configurations and deviations of root canals maxillary first premolars. Oral Surg Oral Med Oral Pathol. 1973 Dec; 36(6): 880-6.

4. Bernaba JM, Madeira MC, Hetem S. Contribuição para o estudo morfológico de raízes e canais do primeiro pré-molar superior humano. Arq Cent Est Fac Odont Univers Minas Gerais. 1965 Jan-Jun; 2(1): 81-92.

5. Moraes IT, Milano NF. Morfologia da cavidade pulpar dos primeiros pré-molares superiores. Rev Fac Odontol Porto Alegre. 1965; 7:11-20.

6. Kerekes K, Tronstad L. Morphometric observations on root canals of human premolars. J Endod. 1977 Feb; 3(2): 74-9.

7. Vertucci FJ, Gegauff A. Root canal morphology of the maxillary first premolar. J Am Dent Assoc. 1979 Aug; 99(2): 194-8.

8. Pinheiro Jr EC, Leite AP, Silva RG, Pécora JD. Pré-molares superiores trirradiculares: anatomia externa e interna. Rev ABO Nac. 1993 Nov-Dez; 1(3): 164-8.

9. Kartal N, Özçelik B, Cimilli H. Root canal morphology of maxillary premolars. J Endod. 1998 Jun; 24(6): 417-9.

10. Chaparro AJ, Segura JJ, Guerrero E, Jiménez-Rubio A, Murillo C, Feito JJ. Number of roots and canals in maxillary first premolars: study of an Andalusian population. Endod Dent Traumatol. 1999 Apr; 2(15): 65-7.

11. Vier FV, Só MVRS, Mattuella LG, Oliveira F, Bozza K, Oliveira EPM. Correlação entre o exame radiográfico e a diafanização na determinação do número de canais em primeiros pré-molares inferiores com e sem sulco longitudinal radicular. Odontologia. Clín.-Científ. Recife. 2004 Jan-Abr; 3(1): 39-48.

12. Sert S, Bayirli GS. Evaluation of the root canal configurations of the mandibular and maxillary permanent teeth by gender in the Turkish population. J Endod. 2004 Jun; 30(6): 391-8.

13. Lu TY, Yang SF, Pai SF. Complicated root canal morphology of mandibular first premolar in a Chinese population using the cross section method. J Endod. 2006 Oct; 32(10): 932-6.

14. Rios LV. Configuração interna dos pré-molares. RGO. 1988 Mar-Abr; 36(2): 101-5.

15. Souza Neto MD, Saquy PC, Aurélio Jr I, Cruz Filho AM, Pécora JD. Primeiro pré-molar superior com três raízes. ROBRAC. 1996 Mar; 6(17): 19-21.

16. Nance R, Tyndall D, Levin LG, Trope M. Identification of root canals in molars by tuned-aperture computed tomography. Int Endod J. 2000 Jul; 33(4): 392-6.

17. Mannocci F, Peru M, Sherriff M, Cook R, Pitt Ford TR. The isthmuses of the mesial root of mandibular molars: a micro-computed tomographic study. Int Endod J. 2005 Aug; 38(8): 558-63.

18. Eder A, Kantor M, Nell A, Moser T, Gahleitner A, Schedle A, Sperr W. Root canal system in the mesiobuccal root of the maxillary first molar: an in vitro comparison study of computed tomography and histology. Dent maxillo fac radiol. 2006 May; 35(3): 175-7.

19. Matherne RP, Angelopoulos C, Kulild JC, Tira D. Use of cone-beam computed tomography to identify root canal systems in vitro. J Endod. 2008 Jan; 34(1): 87-9.

20. Reuben J, Velmurugan N, Kandaswamy D. The evaluation of root canal morphology of the mandibular first molar in an Indian population using spiral computed tomography scan: an in vitro study. J Endod. 2008 Fev. 34(2): 212-5.

21. Sachdeva GS, Ballal S, Gopikrishna V, Kandaswamy D. Endodontic management of a mandibular second premolar with four roots and four root canals with the aid of spiral computed tomography: a case report. J Endod. 2008 Jan; 34(1): 104-7.

22. Abuabara A, Schreiber J, Baratto Filho F, Cruz GV, Guerino L. Análise da anatomia externa no primeiro molar superior por meio da tomografia computadorizada cone beam. Rev sul-bras odontol. 2008 Ago; 5(2): 38-40.

23. Vier-Pelisser FV, Dummer PMH, Bryant S, Marca C, Só MVR, Figueiredo JAP. The anatomy of the root canal system of three-rooted maxillary premolars analysed using high-resolution computed tomography. Int Endod J. 2010 Dec; 43(12): 1122-31.

24. Garib DG, Raymundo Jr. R, Raymundo MV, Raymundo DV, Ferreira SN. Tomografia computadorizada de feixe cônico (Cone beam): entendendo este novo método de diagnóstico por imagem com promissora aplicabilidade na Ortodontia. R Dental Press Ortodon Ortop Facial. 2007 Mar-Abr 2007; 12(2): 139-56.

25. Lima I, Appoloni C, Oliveira L de, Lopes RT. Caracterização de materiais cerâmicos através da microtomografia computadorizada 3D. Rev Bras de Arqueom, Rest e Conserv. 2007; 1(2): 22-7.

26. Robinson S, Suomalainen A, Kortesniemi M. µTC. Eur J Radiol. 2005 Nov; 56(2): 185-91.

27. Plotino G, Grande NM, Pecci R, Bedini R, Pameijer CH, Somma F. Three-dimensional imaging using microcomputed tomography for studying tooth macromorphology. J Am Dent Assoc. 2006 Nov; 137(11):1555-61.

28. Liedke GS, Silveira HED da, Silveira HLD da, Dutra V, Figueiredo JAP de. Influence of voxel size in the diagnostic ability of cone beam tomography to evaluate simulated external root resorption. J Endod. 2009 Fev; 35(2): 233-5.

29. Peters OA, Laib A, Göhring TN, Barbakow F. Changes in root canal geometry after preparation assessed by high-resolution computed tomography. J Endod. 2001 Jan; 27(1): 1-6.

30. Peters OA, Laib A, Rüegsegger P, Barbakow F. Three-dimensional analysis of root canal geometry by high-resolution computed tomography. J Dent Res. 2000 Jun; 79(6): 1405-9.

31. Rhodes JS, Pitt Ford TR, Lynch JA, Liepins PJ, Curtis RV. Micro-computed tomography: a new tool for experimental endodontology. Int Endod J. 1999 May; 32(2): 165-70.

32. Peters OA, Peters CI, Schönenberger K, Barbakow F. ProTaper rotary root canal preparation: effects of canal anatomy on final shape analysed by micro CT. Int Endod J. 2003 Feb; 36(2): 86-92.

33. Bjorndal L, Carlsen O, Thuesen G, Darvann T, Kreiborg S. External and internal macromorphology in 3D-reconstructed maxillary molars using computerized X-ray microtomography. Int Endod J. 1999 Jan; 32(1): 3-9.

34. Lee JK, Ha BH, Choi JH, Heo SM, Perinpanayagam H. Quantitative three-dimensional analysis of root canal curvature in maxillary first molars using micro-computed tomography. J Endod. 2006 Oct; 32(10): 941-5.

35. Gambill JM, Alder M, Del Rio CE. Comparison Of nickel-titanium and stainless hand-file instrumentation using computed tomography. J Endod. 1996 Jul; 22(7): 369-75.

36. Peters OA, Schönenberger K, Laib A. Effects of four Ni-Ti preparation techniques on root canal geometry assessed by micro computed tomography. Int Endod J. 2001 Apr; 34(3): 221-30.

37. Hübscher W, Barbakow F, Peters OA. Root-canal preparation with FlexMaster: canal shapes analysed by micro-computed tomography. Int Endod J. 2003 Nov; 36(11): 740-7.

38. Paqué F, Barbakow F, Peters OA. Root canal preparation with Endo-Eze AET: changes in root canal shape assessed by micro-computed tomography. Int Endod J. 2005 Jul; 38(7): 456-64.

39. Sogur E, Baksi BG, Gröndahl HG. Imaging of root canal fillings: a comparison of subjective image quality between limited cone-beam CT, storage phosphor and film radiography. Int Endod J. 2007 Mar. 40(3): 179-85.

40. Sanfelice CM, Costa FB, Só MVR, Vier-Pelisser F, Bier CAS, Grecca FS. Effects of Four Instruments on Coronal Pre-enlargement by Using Cone Beam Computed Tomography. J Endod. 2010 May; 36(5): 858-61.

41. Maret D, Molinier F, Braga J, Peters AO, Telmon N, Treil J, Inglèse JM, Cossié A, Kahn JL, Sixou M. Accuracy of 3D reconstructions based on cone beam computed tomography. J Dent Res. 2010 Dec; 89(12): 1465-69.

42. Rodrigues AF, Vitral RWF. Aplicações da Tomografia Computadorizada na Odontologia. Pesq Bras Odontoped Clin Integr. 2007 Set-Dez; 7(3): 317-24.

43. Almeida CAM, Schellini AS, Gregório EA, Pelizzon CH. Utilização do AutoCAD 2004 para quantificação de pesquisas usando fotomicrografias eletrônicas. Rev Bras Oftalmol. 2007 Jul-Ago; 66(4): 227-30.

44. Vanzin ACM, Barletta FB, Fontanella V. Comparative assessment of root canal preparation by undergraduate students using manual and automated devices. Rev. odonto ciênc. 2010 Jan-Mar; 25(1):69-73.

45. Oliveira OL. Morfologia externa das raízes de primeiros pré-molares trirradiculares humanos. Arq Cent Est Cur Odontol 1975; 12(1): 203-20.

46. Barton DJ, Clark SJ, Eleazer PD, Scheetz JP, Farman AG. Tuned-aperture computed tomography versus parallax analog and digital radiographic images in detecting second mesiobuccal canals in maxillary first molars. Oral Surg Oral Med Oral Pathol Oral Radiol Endod. 2003 Aug; 96(2): 223-8.

47. Dummer PMH, Mc Ginn J, Rees DG. The position and topography of the apical canal constriction and apical foramen. Int Endod J. 1984 Oct; 17(4): 192-198.

ANEXOS

ANEXO A. PARECER DO COMITÊ DE ÉTICA

Pontifícia Universidade Católica do Rio Grande do Sul
PRÓ-REITORIA DE PESQUISA E PÓS-GRADUAÇÃO
COMITÊ DE ÉTICA EM PESQUISA

OF.CEP-006/11

Porto Alegre, 06 de janeiro de 2011.

Senhor Pesquisador,

O Comitê de Ética em Pesquisa da PUCRS apreciou e aprovou sua solicitação de realizar a parte experimental sem envio de material biológico ao exterior de seu protocolo de pesquisa intitulado **"Estudo da variação da área da câmara pulpar e do canal radicular de pré-molares superiores com três raízes através da microtomografia computadorizada e da tomografia de feixe cônico"**, tendo em vista o prazo de defesa da dissertação de mestrado de sua orientanda Caroline Marca.

O referido protocolo de pesquisa foi aprovado por este CEP em 29 de outubro de 2010 com registro nº 10/05068.

Lembramos que a outra parte do estudo somente poderá ser realizada no exterior com a devida aprovação da CONEP.

Atenciosamente,

Prof. Dr. Rodolfo Herberto Schneider
Coordenador do CEP-PUCRS

Ilmo. Sr.
Prof. Dr. José Antônio Poli de Figueiredo
FO
Nesta Universidade

PUCRS
Campus Central
Av. Ipiranga, 6690 – 3ºandar – CEP: 90610-000
Sala 314 – Fone Fax: (51) 3320-3345
E-mail: cep@pucrs.br
www.pucrs.br/prppg/cep

ANEXO B. SUBMISSÃO

Jose Antonio P de Figueiredo

De:	ees.joe.0.f8e74.7d8e461f@eesmail.elsevier.com em nome de The Journal of Endodontics [JEndodontics@uthscsa.edu]
Enviado em:	quinta-feira, 3 de março de 2011 10:33
Para:	Jose Antonio P de Figueiredo
Assunto:	Submission Confirmation for Variations in cross-sectional area of three-rooted maxillary premolar roots and canals analyzed using high-resolution computed tomography and cone beam tomography

Dear Dr. Figueiredo,

Your submission entitled "Variations in cross-sectional area of three-rooted maxillary premolar roots and canals analyzed using high-resolution computed tomography and cone beam tomography" has been received by the Journal of Endodontics.

You will be able to check on the progress of your paper by logging on to the Journal of Endodontics web site as an author.

The URL is http://ees.elsevier.com/joe/

Your username is: endofig

If you need to retrieve password details, please go to: http://ees.elsevier.com/joe/automail_query.asp

Your manuscript will be given a reference number once an Editor has been assigned.

Thank you for submitting your work to the Journal of Endodontics.

Kind regards,

Journal of Endodontics

OK

03.03.2011

Elsevier Editorial System(tm) for Journal of Endodontics
Manuscript Draft

Manuscript Number:

Title: Variations in cross-sectional area of three-rooted maxillary premolar roots and canals analyzed using high-resolution computed tomography and cone beam tomography

Article Type: Basic Research - Technology

Keywords: root canal anatomy; maxillary premolar; high-resolution computed tomography; cone beam computed tomography

Corresponding Author: Dr Jose Antonio Poli de Figueiredo, PhD

Corresponding Author's Institution: Pontifical Catholic University of Rio Grande do Sul - PUCRS

First Author: Caroline Marca, BDS

Order of Authors: Caroline Marca, BDS; Paul M Dummer, BDS MScD PhD DDSc FDS RCS (Ed) FHEA; Susan Bryant, BDS; Fabiana V Vier Pelisser, BDS, MSc, PhD; Marcus Vinícius R Só, BDS, MSc, PhD; Vania Fontanella, BDS, MSc, PhD; Vinicius D Dutra, BDS, PhD; Jose Antonio Poli de Figueiredo, PhD

Manuscript Region of Origin: Latin & South America

Abstract: Introduction: This study analyzed variations in canal and root cross-sectional area in three-rooted maxillary premolars between high-resolution computed tomography (µCT) and cone beam computed tomography (CBCT). Methods: Sixteen extracted maxillary premolars with three distinct roots and fully formed apices were scanned using µCT and CBCT. Photoshop CS software was used to measure root and canal cross-sectional areas at the most cervical and the most apical points of each root third in images obtained using the two tomographic computed (CT) techniques, and at 30 root sections equidistant from both root ends using µCT images. Canal and root areas were compared between each method using the Student t test for paired samples and 95% confidence intervals. Results: Images using µCT were sharper than those obtained using CBCT. There were statistically significant differences in mean area measurements of roots and canals between the µCT and CBCT techniques ($p<0.05$) Root and canal areas had similar variations in cross-sectional µCT images and became proportionally smaller in a cervical to apical direction as the cementodentinal junction was approached, from where the area then increased apically. Conclusion: Although variation was similar in the roots and canals under study, CBCT produced poorer image details than µCT.

ANEXO C. ESTATÍSTICA

C.1 ANÁLISE ESTATÍSTICA DA COMPARAÇÃO DOS MÉTODOS TOMOGRÁFICOS

```
GET
  FILE='C:\Users\WAGNER01\Consultorias\Cons2010\CarolineMarca\ARQ-CM09.sav
'.

>Warning # 67.  Command name: GET FILE
>The document is already in use by another user or process.  If you make
>changes to the document they may overwrite changes made by others or your
>changes may be overwritten by others.
>File opened C:\Users\WAGNER01\Consultorias\Cons2010\CarolineMarca\ARQ-CM0
9.sav
DATASET NAME DataSet1 WINDOW=FRONT.
```

Dataset Name

Warnings

The active dataset will replace the existing dataset named DataSet1.

```
if (dente=13) m2x1t2c=0.6092.
if (dente=13) m2x1t2m=0.43.
if (dente=13) m2x1t2d=0.3583.
***** RAIZES.
DATASET ACTIVATE DataSet1.
T-TEST PAIRS=
  M1R1T1M M1R1T2M M1R1T3M M1R2T1M M1R2T2M M1R2T3M M1R3T1M M1R3T2M M1R3T3M
  WITH
  M2R1T1M M2R1T2M M2R1T3M M2R2T1M M2R2T2M M2R2T3M M2R3T1M M2R3T2M M2R3T3M
 (PAIRED)
  /CRITERIA=CI(.9500)
  /MISSING=ANALYSIS.
```

T-Test

```
[DataSet1] C:\Users\WAGNER01\Consultorias\Cons2010\CarolineMarca\ARQ-CM09.
sav
```

Paired Samples Statistics

		Mean	N	Std. Deviation	Std. Error Mean
Pair 1	M1R1T1M	13,337062	16	2,7984888	,6996222
	M2R1T1M	11,261738	16	2,4314345	,6078586
Pair 2	M1R1T2M	9,421841	16	2,1640409	,5410102
	M2R1T2M	8,251744	16	1,8042040	,4510510
Pair 3	M1R1T3M	4,680163	16	1,2330715	,3082679
	M2R1T3M	5,287650	16	1,3216227	,3304057
Pair 4	M1R2T1M	7,541394	16	1,7801759	,4450440
	M2R2T1M	6,154375	16	1,2912981	,3228245

Paired Samples Statistics

		Mean	N	Std. Deviation	Std. Error Mean
Pair 5	M1R2T2M	5,221438	16	1,2496282	,3124070
	M2R2T2M	4,824044	16	,9751875	,2437969
Pair 6	M1R2T3M	2,613263	16	,7668590	,1917148
	M2R2T3M	3,557569	16	,8812835	,2203209
Pair 7	M1R3T1M	6,691900	16	1,7737257	,4434314
	M2R3T1M	5,475781	16	1,3010206	,3252552
Pair 8	M1R3T2M	4,712019	16	1,4037499	,3509375
	M2R3T2M	4,383981	16	1,0349880	,2587470
Pair 9	M1R3T3M	2,432444	16	,9721349	,2430337
	M2R3T3M	3,267550	16	,8098986	,2024746

Paired Samples Correlations

		N	Correlation	Sig.
Pair 1	M1R1T1M & M2R1T1M	16	,922	,000
Pair 2	M1R1T2M & M2R1T2M	16	,967	,000
Pair 3	M1R1T3M & M2R1T3M	16	,843	,000
Pair 4	M1R2T1M & M2R2T1M	16	,959	,000
Pair 5	M1R2T2M & M2R2T2M	16	,931	,000
Pair 6	M1R2T3M & M2R2T3M	16	,584	,018
Pair 7	M1R3T1M & M2R3T1M	16	,859	,000
Pair 8	M1R3T2M & M2R3T2M	16	,772	,000
Pair 9	M1R3T3M & M2R3T3M	16	,476	,062

Paired Samples Test

		Paired Differences		
		Mean	Std. Deviation	Std. Error Mean
Pair 1	M1R1T1M - M2R1T1M	2,0753250	1,0965949	,2741487
Pair 2	M1R1T2M - M2R1T2M	1,1700972	,6212482	,1553120
Pair 3	M1R1T3M - M2R1T3M	-,6074875	,7211805	,1802951
Pair 4	M1R2T1M - M2R2T1M	1,3870187	,6526913	,1631728
Pair 5	M1R2T2M - M2R2T2M	,3973938	,4941366	,1235342
Pair 6	M1R2T3M - M2R2T3M	-,9443063	,7588741	,1897185
Pair 7	M1R3T1M - M2R3T1M	1,2161188	,9359068	,2339767
Pair 8	M1R3T2M - M2R3T2M	,3280375	,8933660	,2233415
Pair 9	M1R3T3M - M2R3T3M	-,8351062	,9229319	,2307330

Paired Samples Test

		Paired Differences 95% Confidence Interval of the Difference Lower	Upper
Pair 1	M1R1T1M - M2R1T1M	1,4909908	2,6596592
Pair 2	M1R1T2M - M2R1T2M	,8390574	1,5011370
Pair 3	M1R1T3M - M2R1T3M	-,9917775	-,2231975
Pair 4	M1R2T1M - M2R2T1M	1,0392241	1,7348134
Pair 5	M1R2T2M - M2R2T2M	,1340869	,6607006
Pair 6	M1R2T3M - M2R2T3M	-1,3486817	-,5399308
Pair 7	M1R3T1M - M2R3T1M	,7174092	1,7148283
Pair 8	M1R3T2M - M2R3T2M	-,1480036	,8040786
Pair 9	M1R3T3M - M2R3T3M	-1,3269019	-,3433106

Paired Samples Test

		t	df	Sig. (2-tailed)
Pair 1	M1R1T1M - M2R1T1M	7,570	15	,000
Pair 2	M1R1T2M - M2R1T2M	7,534	15	,000
Pair 3	M1R1T3M - M2R1T3M	-3,369	15	,004
Pair 4	M1R2T1M - M2R2T1M	8,500	15	,000
Pair 5	M1R2T2M - M2R2T2M	3,217	15	,006
Pair 6	M1R2T3M - M2R2T3M	-4,977	15	,000
Pair 7	M1R3T1M - M2R3T1M	5,198	15	,000
Pair 8	M1R3T2M - M2R3T2M	1,469	15	,163
Pair 9	M1R3T3M - M2R3T3M	-3,619	15	,003

```
T-TEST PAIRS=
  M1R1T1D M1R1T2D M1R1T3D M1R2T1D M1R2T2D M1R2T3D M1R3T1D M1R3T2D M1R3T3D
  WITH
  M2R1T1D M2R1T2D M2R1T3D M2R2T1D M2R2T2D M2R2T3D M2R3T1D M2R3T2D M2R3T3D
 (PAIRED)
  /CRITERIA=CI(.9500)
  /MISSING=ANALYSIS.
```

T-Test

```
[DataSet1] C:\Users\WAGNER01\Consultorias\Cons2010\CarolineMarca\ARQ-CM09.
sav
```

Paired Samples Statistics

		Mean	N	Std. Deviation	Std. Error Mean
Pair 1	M1R1T1D	4,268256	16	2,0490903	,5122726
	M2R1T1D	3,173494	16	1,7996721	,4499180

Paired Samples Statistics

		Mean	N	Std. Deviation	Std. Error Mean
Pair 2	M1R1T2D	3,330101	16	1,2963320	,3240830
	M2R1T2D	2,165675	16	1,3746194	,3436549
Pair 3	M1R1T3D	6,078469	16	2,2026681	,5506670
	M2R1T3D	3,108544	16	1,5617985	,3904496
Pair 4	M1R2T1D	2,498975	16	1,6055653	,4013913
	M2R2T1D	1,428856	16	,9685054	,2421264
Pair 5	M1R2T2D	2,065938	16	,6784373	,1696093
	M2R2T2D	,904800	16	,5410035	,1352509
Pair 6	M1R2T3D	3,095313	16	1,0249137	,2562284
	M2R2T3D	1,175769	16	,6770156	,1692539
Pair 7	M1R3T1D	1,961894	16	1,3242531	,3310633
	M2R3T1D	1,146663	16	,7626037	,1906509
Pair 8	M1R3T2D	1,912431	16	,6359214	,1589803
	M2R3T2D	,566619	16	,6491209	,1622802
Pair 9	M1R3T3D	2,511281	16	,8165612	,2041403
	M2R3T3D	,985412	16	,6372581	,1593145

Paired Samples Correlations

		N	Correlation	Sig.
Pair 1	M1R1T1D & M2R1T1D	16	,792	,000
Pair 2	M1R1T2D & M2R1T2D	16	,793	,000
Pair 3	M1R1T3D & M2R1T3D	16	,763	,001
Pair 4	M1R2T1D & M2R2T1D	16	,802	,000
Pair 5	M1R2T2D & M2R2T2D	16	,029	,916
Pair 6	M1R2T3D & M2R2T3D	16	,596	,015
Pair 7	M1R3T1D & M2R3T1D	16	,463	,071
Pair 8	M1R3T2D & M2R3T2D	16	-,023	,932
Pair 9	M1R3T3D & M2R3T3D	16	,471	,066

Paired Samples Test

		Paired Differences		
		Mean	Std. Deviation	Std. Error Mean
Pair 1	M1R1T1D - M2R1T1D	1,0947625	1,2642555	,3160639
Pair 2	M1R1T2D - M2R1T2D	1,1644256	,8629852	,2157463
Pair 3	M1R1T3D - M2R1T3D	2,9699250	1,4277594	,3569398
Pair 4	M1R2T1D - M2R2T1D	1,0701188	1,0113240	,2528310
Pair 5	M1R2T2D - M2R2T2D	1,1611375	,8554980	,2138745
Pair 6	M1R2T3D - M2R2T3D	1,9195438	,8256313	,2064078
Pair 7	M1R3T1D - M2R3T1D	,8152313	1,1828881	,2957220
Pair 8	M1R3T2D - M2R3T2D	1,3458125	,9191481	,2297870
Pair 9	M1R3T3D - M2R3T3D	1,5258687	,7635859	,1908965

Paired Samples Test

		Paired Differences: 95% Confidence Interval of the Difference	
		Lower	Upper
Pair 1	M1R1T1D - M2R1T1D	,4210883	1,7684367
Pair 2	M1R1T2D - M2R1T2D	,7045733	1,6242780
Pair 3	M1R1T3D - M2R1T3D	2,2091257	3,7307243
Pair 4	M1R2T1D - M2R2T1D	,5312222	1,6090153
Pair 5	M1R2T2D - M2R2T2D	,7052748	1,6170002
Pair 6	M1R2T3D - M2R2T3D	1,4795959	2,3594916
Pair 7	M1R3T1D - M2R3T1D	,1849147	1,4455478
Pair 8	M1R3T2D - M2R3T2D	,8560330	1,8355920
Pair 9	M1R3T3D - M2R3T3D	1,1189826	1,9327549

Paired Samples Test

		t	df	Sig. (2-tailed)
Pair 1	M1R1T1D - M2R1T1D	3,464	15	,003
Pair 2	M1R1T2D - M2R1T2D	5,397	15	,000
Pair 3	M1R1T3D - M2R1T3D	8,321	15	,000
Pair 4	M1R2T1D - M2R2T1D	4,233	15	,001
Pair 5	M1R2T2D - M2R2T2D	5,429	15	,000
Pair 6	M1R2T3D - M2R2T3D	9,300	15	,000
Pair 7	M1R3T1D - M2R3T1D	2,757	15	,015
Pair 8	M1R3T2D - M2R3T2D	5,857	15	,000
Pair 9	M1R3T3D - M2R3T3D	7,993	15	,000

```
***** CANAIS.
DATASET ACTIVATE DataSet1.
T-TEST PAIRS=
  M1X1T1M M1X1T2M M1X1T3M M1X2T1M M1X2T2M M1X2T3M M1X3T1M M1X3T2M M1X3T3M
  WITH
  M2X1T1M M2X1T2M M2X1T3M M2X2T1M M2X2T2M M2X2T3M M2X3T1M M2X3T2M M2X3T3M
 (PAIRED)
  /CRITERIA=CI(.9500)
  /MISSING=ANALYSIS.
```

T-Test

```
[DataSet1] C:\Users\WAGNER01\Consultorias\Cons2010\CarolineMarca\ARQ-CM09.
sav
```

Paired Samples Statistics

		Mean	N	Std. Deviation	Std. Error Mean
Pair 1	M1X1T1M	,954419	16	,3852100	,0963025
	M2X1T1M	,898056	16	,3112804	,0778201
Pair 2	M1X1T2M	,394819	16	,1573462	,0393366
	M2X1T2M	,541975	16	,2127495	,0531874
Pair 3	M1X1T3M	,169713	16	,0737076	,0184269
	M2X1T3M	,298981	16	,1247684	,0311921
Pair 4	M1X2T1M	,314425	16	,1716169	,0429042
	M2X2T1M	,378487	16	,1805689	,0451422
Pair 5	M1X2T2M	,144856	16	,0665874	,0166469
	M2X2T2M	,269862	16	,1319041	,0329760
Pair 6	M1X2T3M	,064813	16	,0319045	,0079761
	M2X2T3M	,178037	16	,0902819	,0225705
Pair 7	M1X3T1M	,216838	16	,1253644	,0313411
	M2X3T1M	,320250	16	,1808164	,0452041
Pair 8	M1X3T2M	,125838	16	,0698933	,0174733
	M2X3T2M	,244106	16	,1232415	,0308104
Pair 9	M1X3T3M	,060800	16	,0373003	,0093251
	M2X3T3M	,171312	16	,0803867	,0200967

Paired Samples Correlations

		N	Correlation	Sig.
Pair 1	M1X1T1M & M2X1T1M	16	,785	,000
Pair 2	M1X1T2M & M2X1T2M	16	,658	,006
Pair 3	M1X1T3M & M2X1T3M	16	,490	,054
Pair 4	M1X2T1M & M2X2T1M	16	,814	,000
Pair 5	M1X2T2M & M2X2T2M	16	,628	,009
Pair 6	M1X2T3M & M2X2T3M	16	,419	,106
Pair 7	M1X3T1M & M2X3T1M	16	,891	,000
Pair 8	M1X3T2M & M2X3T2M	16	,703	,002
Pair 9	M1X3T3M & M2X3T3M	16	,729	,001

Paired Samples Test

		Paired Differences		
		Mean	Std. Deviation	Std. Error Mean
Pair 1	M1X1T1M - M2X1T1M	,0563625	,2385860	,0596465
Pair 2	M1X1T2M - M2X1T2M	-,1471563	,1612142	,0403036
Pair 3	M1X1T3M - M2X1T3M	-,1292687	,1094595	,0273649
Pair 4	M1X2T1M - M2X2T1M	-,0640625	,1078679	,0269670
Pair 5	M1X2T2M - M2X2T2M	-,1250062	,1038897	,0259724
Pair 6	M1X2T3M - M2X2T3M	-,1132250	,0821751	,0205438
Pair 7	M1X3T1M - M2X3T1M	-,1034125	,0896502	,0224125

Paired Samples Test

		Paired Differences: 95% Confidence Interval of the Difference	
		Lower	Upper
Pair 1	M1X1T1M - M2X1T1M	-,0707710	,1834960
Pair 2	M1X1T2M - M2X1T2M	-,2330612	-,0612513
Pair 3	M1X1T3M - M2X1T3M	-,1875956	-,0709419
Pair 4	M1X2T1M - M2X2T1M	-,1215412	-,0065838
Pair 5	M1X2T2M - M2X2T2M	-,1803652	-,0696473
Pair 6	M1X2T3M - M2X2T3M	-,1570130	-,0694370
Pair 7	M1X3T1M - M2X3T1M	-,1511837	-,0556413

Paired Samples Test

		t	df	Sig. (2-tailed)
Pair 1	M1X1T1M - M2X1T1M	,945	15	,360
Pair 2	M1X1T2M - M2X1T2M	-3,651	15	,002
Pair 3	M1X1T3M - M2X1T3M	-4,724	15	,000
Pair 4	M1X2T1M - M2X2T1M	-2,376	15	,031
Pair 5	M1X2T2M - M2X2T2M	-4,813	15	,000
Pair 6	M1X2T3M - M2X2T3M	-5,511	15	,000
Pair 7	M1X3T1M - M2X3T1M	-4,614	15	,000

Paired Samples Test

		Paired Differences		
		Mean	Std. Deviation	Std. Error Mean
Pair 8	M1X3T2M - M2X3T2M	-,1182687	,0892493	,0223123
Pair 9	M1X3T3M - M2X3T3M	-,1105125	,0589851	,0147463

Paired Samples Test

		Paired Differences: 95% Confidence Interval of the Difference	
		Lower	Upper
Pair 8	M1X3T2M - M2X3T2M	-,1658263	-,0707112
Pair 9	M1X3T3M - M2X3T3M	-,1419434	-,0790816

Paired Samples Test

		t	df	Sig. (2-tailed)
Pair 8	M1X3T2M - M2X3T2M	-5,301	15	,000
Pair 9	M1X3T3M - M2X3T3M	-7,494	15	,000

```
T-TEST PAIRS=
  M1X1T1D M1X1T2D M1X1T3D M1X2T1D M1X2T2D M1X2T3D M1X3T1D M1X3T2D M1X3T3D
  WITH
  M2X1T1D M2X1T2D M2X1T3D M2X2T1D M2X2T2D M2X2T3D M2X3T1D M2X3T2D M2X3T3D
 (PAIRED)
  /CRITERIA=CI(.9500)
  /MISSING=ANALYSIS.
```

T-Test

```
[DataSet1] C:\Users\WAGNER01\Consultorias\Cons2010\CarolineMarca\ARQ-CM09.
sav
```

Paired Samples Statistics

		Mean	N	Std. Deviation	Std. Error Mean
Pair 1	M1X1T1D	,896388	16	,4541153	,1135288
	M2X1T1D	,591250	16	,3486501	,0871625
Pair 2	M1X1T2D	,217725	16	,1788895	,0447224
	M2X1T2D	,152294	16	,1673136	,0418284
Pair 3	M1X1T3D	,185344	16	,1409000	,0352250
	M2X1T3D	,239637	16	,2092353	,0523088
Pair 4	M1X2T1D	,230462	16	,2157148	,0539287
	M2X2T1D	,089575	16	,1421428	,0355357
Pair 5	M1X2T2D	,099125	16	,0544913	,0136228
	M2X2T2D	,038069	16	,0497755	,0124439
Pair 6	M1X2T3D	,053363	16	,0411426	,0102857
	M2X2T3D	,069438	16	,0768215	,0192054
Pair 7	M1X3T1D	,097381	16	,1201934	,0300483
	M2X3T1D	,071669	16	,1255070	,0313768
Pair 8	M1X3T2D	,084656	16	,0619342	,0154836
	M2X3T2D	,044800	16	,0634306	,0158577
Pair 9	M1X3T3D	,038669	16	,0432382	,0108095
	M2X3T3D	,055981	16	,0795604	,0198901

Paired Samples Correlations

		N	Correlation	Sig.
Pair 1	M1X1T1D & M2X1T1D	16	,841	,000
Pair 2	M1X1T2D & M2X1T2D	16	,309	,245
Pair 3	M1X1T3D & M2X1T3D	16	,642	,007
Pair 4	M1X2T1D & M2X2T1D	16	,455	,077
Pair 5	M1X2T2D & M2X2T2D	16	,332	,209
Pair 6	M1X2T3D & M2X2T3D	16	,265	,321
Pair 7	M1X3T1D & M2X3T1D	16	,246	,358
Pair 8	M1X3T2D & M2X3T2D	16	-,330	,212
Pair 9	M1X3T3D & M2X3T3D	16	,486	,056

Paired Samples Test

		Paired Differences		
		Mean	Std. Deviation	Std. Error Mean
Pair 1	M1X1T1D - M2X1T1D	,3051375	,2476536	,0619134
Pair 2	M1X1T2D - M2X1T2D	,0654312	,2037826	,0509456
Pair 3	M1X1T3D - M2X1T3D	-,0542937	,1605254	,0401313
Pair 4	M1X2T1D - M2X2T1D	,1408875	,1970875	,0492719
Pair 5	M1X2T2D - M2X2T2D	,0610562	,0603745	,0150936
Pair 6	M1X2T3D - M2X2T3D	-,0160750	,0769368	,0192342
Pair 7	M1X3T1D - M2X3T1D	,0257125	,1509195	,0377299
Pair 8	M1X3T2D - M2X3T2D	,0398563	,1022462	,0255616
Pair 9	M1X3T3D - M2X3T3D	-,0173125	,0696926	,0174232

Paired Samples Test

		Paired Differences	
		95% Confidence Interval of the Difference	
		Lower	Upper
Pair 1	M1X1T1D - M2X1T1D	,1731722	,4371028
Pair 2	M1X1T2D - M2X1T2D	-,0431568	,1740193
Pair 3	M1X1T3D - M2X1T3D	-,1398317	,0312442
Pair 4	M1X2T1D - M2X2T1D	,0358670	,2459080
Pair 5	M1X2T2D - M2X2T2D	,0288850	,0932275
Pair 6	M1X2T3D - M2X2T3D	-,0570717	,0249217
Pair 7	M1X3T1D - M2X3T1D	-,0547068	,1061318
Pair 8	M1X3T2D - M2X3T2D	-,0146269	,0943394
Pair 9	M1X3T3D - M2X3T3D	-,0544491	,0198241

Paired Samples Test

		t	df	Sig. (2-tailed)
Pair 1	M1X1T1D - M2X1T1D	4,928	15	,000
Pair 2	M1X1T2D - M2X1T2D	1,284	15	,219
Pair 3	M1X1T3D - M2X1T3D	-1,353	15	,196
Pair 4	M1X2T1D - M2X2T1D	2,859	15	,012
Pair 5	M1X2T2D - M2X2T2D	4,045	15	,001
Pair 6	M1X2T3D - M2X2T3D	-,836	15	,416
Pair 7	M1X3T1D - M2X3T1D	,681	15	,506
Pair 8	M1X3T2D - M2X3T2D	1,559	15	,140
Pair 9	M1X3T3D - M2X3T3D	-,994	15	,336

```
SAVE OUTFILE='C:\Users\WAGNER01\Consultorias\Cons2010\CarolineMarca\ARQ-CM
10.sav'
  /COMPRESSED.
```

C.2 ANÁLISE ESTATÍSTICA DA VARIAÇÃO DA PROPORÇÃO DE ÁREA DE CANAL EM RELAÇÃO A RAIZ

```
GET
  FILE=
    'C:\Users\Mario\Documents\DocsMario\A01-Cons\MWC\Cons2010\CarolineMarc
a\ARQ-CM-TRACADO-V02.sav'.
DATASET NAME DataSet1 WINDOW=FRONT.
DATASET ACTIVATE DataSet1.
FREQUENCIES VARIABLES=PC01X1T1 PC02X1T1 PC03X1T1 PC04X1T1 PC05X1T1 PC06X1T
1 PC07X1T1 PC08X1T1
    PC09X1T1 PC10X1T1 PC01X1T2 PC02X1T2 PC03X1T2 PC04X1T2 PC05X1T2 PC06X1T
2 PC07X1T2 PC08X1T2 PC09X1T2
    PC10X1T2 PC01X1T3 PC02X1T3 PC03X1T3 PC04X1T3 PC05X1T3 PC06X1T3 PC07X1T
3 PC08X1T3 PC09X1T3 PC10X1T3
    PC01X2T1 PC02X2T1 PC03X2T1 PC04X2T1 PC05X2T1 PC06X2T1 PC07X2T1 PC08X2T
1 PC09X2T1 PC10X2T1 PC01X2T2
    PC02X2T2 PC03X2T2 PC04X2T2 PC05X2T2 PC06X2T2 PC07X2T2 PC08X2T2 PC09X2T
2 PC10X2T2 PC01X2T3 PC02X2T3
    PC03X2T3 PC04X2T3 PC05X2T3 PC06X2T3 PC07X2T3 PC08X2T3 PC09X2T3 PC10X2T
3 PC01X3T1 PC02X3T1 PC03X3T1
    PC04X3T1 PC05X3T1 PC06X3T1 PC07X3T1 PC08X3T1 PC09X3T1 PC10X3T1 PC01X3T
2 PC02X3T2 PC03X3T2 PC04X3T2
    PC05X3T2 PC06X3T2 PC07X3T2 PC08X3T2 PC09X3T2 PC10X3T2 PC01X3T3 PC02X3T
3 PC03X3T3 PC04X3T3 PC05X3T3
    PC06X3T3 PC07X3T3 PC08X3T3 PC09X3T3 PC10X3T3
  /STATISTICS=STDDEV MINIMUM MAXIMUM MEAN
  /ORDER=ANALYSIS/FORMAT=NOTABLE.
```

Frequencies

[DataSet1] C:\Users\Mario\Documents\DocsMario\A01-Cons\MWC\Cons2010\CarolineMarca\ARQ-CM-TRACADO-V02.sav

Statistics

		PC01X1T1	PC02X1T1	PC03X1T1	PC04X1T1	PC05X1T1
N	Valid	16	16	16	16	16
	Missing	3	3	3	3	3
	Mean	8,301695	6,684270	5,911754	5,427081	5,028065
	Std. Deviation	2,3470017	1,9109611	1,7509381	1,8822273	1,8889115
	Minimum	4,2464	4,0366	3,3169	2,7463	2,3395
	Maximum	12,8410	11,5746	10,5124	10,3673	9,4265

Statistics

		PC06X1T1	PC07X1T1	PC08X1T1	PC09X1T1	PC10X1T1
N	Valid	16	16	16	16	16
	Missing	3	3	3	3	3
	Mean	4,898113	4,764401	4,584885	4,487337	4,290863
	Std. Deviation	1,9053059	1,7748015	1,6263514	1,5244053	1,4415466
	Minimum	2,1866	2,2342	2,0606	2,3206	2,2686
	Maximum	9,0792	8,9081	8,4816	7,9640	6,9972

Statistics

		PC01X1T2	PC02X1T2	PC03X1T2	PC04X1T2	PC05X1T2
N	Valid	16	16	16	16	16
	Missing	3	3	3	3	3
	Mean	4,236112	4,180901	4,046953	4,043757	4,058190
	Std. Deviation	1,4379383	1,4222113	1,5657664	1,5880071	1,5591595
	Minimum	1,7139	1,4170	,9090	,8844	,9319
	Maximum	6,6848	6,7127	6,5982	6,8214	6,9021

Statistics

		PC06X1T2	PC07X1T2	PC08X1T2	PC09X1T2	PC10X1T2
N	Valid	16	16	16	16	16
	Missing	3	3	3	3	3
	Mean	3,906259	3,863886	3,800454	3,557368	3,515126
	Std. Deviation	1,5951383	1,7249508	1,7097257	1,6801392	1,6889102
	Minimum	,8022	,8110	1,0278	1,0943	,8783
	Maximum	6,9199	7,1103	7,2365	7,0086	7,2062

Statistics

		PC01X1T3	PC02X1T3	PC03X1T3	PC04X1T3	PC05X1T3
N	Valid	16	16	16	16	16
	Missing	3	3	3	3	3
	Mean	3,307049	3,080507	2,923361	2,775906	2,670548
	Std. Deviation	1,7991258	1,8654633	1,9232285	1,8204132	1,6878743
	Minimum	1,0864	,7530	,5479	,6168	,5152
	Maximum	7,7039	7,5472	7,5803	6,6648	6,0916

Statistics

		PC06X1T3	PC07X1T3	PC08X1T3	PC09X1T3	PC10X1T3
N	Valid	16	16	16	16	16
	Missing	3	3	3	3	3
	Mean	2,563398	2,331343	2,435386	2,668094	4,707915
	Std. Deviation	1,6597106	1,5299921	1,2967245	1,1048266	1,9280190
	Minimum	,5412	,6330	,6282	1,1977	2,0874
	Maximum	6,0568	5,4463	4,8131	4,3088	9,7069

Statistics

		PC01X2T1	PC02X2T1	PC03X2T1	PC04X2T1	PC05X2T1
N	Valid	16	16	16	16	16
	Missing	3	3	3	3	3
	Mean	4,443030	3,495599	3,144435	2,806316	2,658256
	Std. Deviation	1,8252421	1,4669316	1,3647787	1,2643298	1,1902732
	Minimum	1,2128	1,1571	1,1767	1,1413	1,0312
	Maximum	7,6598	5,9373	5,8559	5,3069	5,1590

Statistics

		PC06X2T1	PC07X2T1	PC08X2T1	PC09X2T1	PC10X2T1
N	Valid	16	16	16	16	16
	Missing	3	3	3	3	3
	Mean	2,654546	2,843981	2,977042	3,027269	3,057249
	Std. Deviation	1,0879805	1,0272846	,9603266	1,0199636	1,0859836
	Minimum	1,4656	1,6007	1,4919	1,4040	1,4005
	Maximum	5,1641	5,0307	5,0291	4,7834	5,0136

Statistics

		PC01X2T2	PC02X2T2	PC03X2T2	PC04X2T2	PC05X2T2
N	Valid	16	16	16	16	16
	Missing	3	3	3	3	3
	Mean	3,042065	3,040993	2,932513	2,865668	2,784789
	Std. Deviation	1,1895070	1,2887121	1,2847087	1,3723544	1,4740973
	Minimum	1,2033	1,0332	1,0081	,8825	,7614
	Maximum	4,7335	5,0208	4,7730	5,1461	5,2338

Statistics

		PC06X2T2	PC07X2T2	PC08X2T2	PC09X2T2	PC10X2T2
N	Valid	16	16	16	16	16
	Missing	3	3	3	3	3
	Mean	2,629589	2,473439	2,314565	2,415523	2,347188
	Std. Deviation	1,3826382	1,4121264	1,2886610	1,4304229	1,4829528
	Minimum	,7227	,6973	,6285	,6706	,6631
	Maximum	5,1229	4,8662	4,6324	5,2770	5,2762

Statistics

		PC01X2T3	PC02X2T3	PC03X2T3	PC04X2T3	PC05X2T3
N	Valid	16	16	16	16	16
	Missing	3	3	3	3	3
	Mean	2,307948	2,207470	2,136508	2,082487	2,073812
	Std. Deviation	1,5403511	1,6005380	1,4491573	1,3984973	1,3612703
	Minimum	,5661	,4444	,6498	,5947	,5847
	Maximum	5,5161	5,6758	5,3435	4,9722	5,0627

Statistics

		PC06X2T3	PC07X2T3	PC08X2T3	PC09X2T3	PC10X2T3
N	Valid	16	16	16	16	16
	Missing	3	3	3	3	3
Mean		2,040964	2,306634	2,241906	2,900357	4,734107
Std. Deviation		1,4156468	1,5969359	1,8937325	2,2893941	4,0178465
Minimum		,5417	,4753	,6404	,7559	,6245
Maximum		5,3731	5,4039	6,2245	8,6319	15,8371

Statistics

		PC01X3T1	PC02X3T1	PC03X3T1	PC04X3T1	PC05X3T1
N	Valid	16	16	16	16	16
	Missing	3	3	3	3	3
Mean		3,322506	2,528306	2,365751	2,407253	2,379726
Std. Deviation		1,3619903	1,0777655	,9160564	,8249307	,7771101
Minimum		1,3492	,7385	,8859	,9439	1,0058
Maximum		6,2725	5,1811	4,6292	4,4888	4,3461

Statistics

		PC06X3T1	PC07X3T1	PC08X3T1	PC09X3T1	PC10X3T1
N	Valid	16	16	16	16	16
	Missing	3	3	3	3	3
Mean		2,363699	2,479910	2,489736	2,539704	2,680054
Std. Deviation		,7883418	,9352831	,9896437	1,0222465	1,0314112
Minimum		,8703	,8368	,7201	1,1460	1,1553
Maximum		4,2112	4,4261	4,5361	4,7082	4,8776

Statistics

		PC01X3T2	PC02X3T2	PC03X3T2	PC04X3T2	PC05X3T2
N	Valid	16	16	16	16	16
	Missing	3	3	3	3	3
Mean		2,706153	2,520384	2,514130	2,406894	2,306631
Std. Deviation		1,0987040	1,0420537	1,1529330	1,1421329	1,1006371
Minimum		,9263	,8708	,9053	,8373	,8342
Maximum		4,9722	4,7138	4,9646	4,8998	4,7212

Statistics

		PC06X3T2	PC07X3T2	PC08X3T2	PC09X3T2	PC10X3T2
N	Valid	16	16	16	16	16
	Missing	3	3	3	3	3
Mean		2,263676	2,143115	2,050831	2,120636	1,947274
Std. Deviation		1,0696133	1,1450463	1,0705076	1,0231930	1,0193580
Minimum		,8859	,7448	,6377	,6558	,5430
Maximum		4,4525	4,5548	4,0830	3,6558	3,8907

Statistics

		PC01X3T3	PC02X3T3	PC03X3T3	PC04X3T3	PC05X3T3
N	Valid	16	16	16	16	16
	Missing	3	3	3	3	3
	Mean	1,983883	1,962474	1,982679	2,025269	2,023726
	Std. Deviation	1,0891894	1,1319546	1,0957576	1,2619872	1,2652678
	Minimum	,3258	,5443	,7425	,4853	,6033
	Maximum	4,0473	4,4217	4,5477	4,8426	4,8487

Statistics

		PC06X3T3	PC07X3T3	PC08X3T3	PC09X3T3	PC10X3T3
N	Valid	16	16	16	16	16
	Missing	3	3	3	3	3
	Mean	2,218909	2,409717	2,590641	3,167480	5,215004
	Std. Deviation	1,4342058	1,4872943	1,5177616	2,1376788	4,2698381
	Minimum	,5484	,7766	,8344	1,1442	1,6860
	Maximum	5,4765	5,8256	6,3561	8,0886	19,1667

```
T-TEST
  /TESTVAL=0
  /MISSING=ANALYSIS
  /VARIABLES=PC01X1T1 PC02X1T1 PC03X1T1 PC04X1T1 PC05X1T1 PC06X1T1 PC07X1T
1 PC08X1T1 PC09X1T1
    PC10X1T1 PC01X1T2 PC02X1T2 PC03X1T2 PC04X1T2 PC05X1T2 PC06X1T2 PC07X1T
2 PC08X1T2 PC09X1T2 PC10X1T2
    PC01X1T3 PC02X1T3 PC03X1T3 PC04X1T3 PC05X1T3 PC06X1T3 PC07X1T3 PC08X1T
3 PC09X1T3 PC10X1T3 PC01X2T1
    PC02X2T1 PC03X2T1 PC04X2T1 PC05X2T1 PC06X2T1 PC07X2T1 PC08X2T1 PC09X2T
1 PC10X2T1 PC01X2T2 PC02X2T2
    PC03X2T2 PC04X2T2 PC05X2T2 PC06X2T2 PC07X2T2 PC08X2T2 PC09X2T2 PC10X2T
2 PC01X2T3 PC02X2T3 PC03X2T3
    PC04X2T3 PC05X2T3 PC06X2T3 PC07X2T3 PC08X2T3 PC09X2T3 PC10X2T3 PC01X3T
1 PC02X3T1 PC03X3T1 PC04X3T1
    PC05X3T1 PC06X3T1 PC07X3T1 PC08X3T1 PC09X3T1 PC10X3T1 PC01X3T2 PC02X3T
2 PC03X3T2 PC04X3T2 PC05X3T2
    PC06X3T2 PC07X3T2 PC08X3T2 PC09X3T2 PC10X3T2 PC01X3T3 PC02X3T3 PC03X3T
3 PC04X3T3 PC05X3T3 PC06X3T3
    PC07X3T3 PC08X3T3 PC09X3T3 PC10X3T3
  /CRITERIA=CI(.95).
```

T-Test

```
[DataSet1] C:\Users\Mario\Documents\DocsMario\A01-Cons\MWC\Cons2010\Caroli
neMarca\ARQ-CM-TRACADO-V02.sav
```

One-Sample Statistics

	N	Mean	Std. Deviation	Std. Error Mean
PC01X1T1	16	8,301695	2,3470017	,5867504
PC02X1T1	16	6,684270	1,9109611	,4777403
PC03X1T1	16	5,911754	1,7509381	,4377345
PC04X1T1	16	5,427081	1,8822273	,4705568
PC05X1T1	16	5,028065	1,8889115	,4722279
PC06X1T1	16	4,898113	1,9053059	,4763265
PC07X1T1	16	4,764401	1,7748015	,4437004
PC08X1T1	16	4,584885	1,6263514	,4065878
PC09X1T1	16	4,487337	1,5244053	,3811013
PC10X1T1	16	4,290863	1,4415466	,3603866
PC01X1T2	16	4,236112	1,4379383	,3594846
PC02X1T2	16	4,180901	1,4222113	,3555528
PC03X1T2	16	4,046953	1,5657664	,3914416
PC04X1T2	16	4,043757	1,5880071	,3970018
PC05X1T2	16	4,058190	1,5591595	,3897899
PC06X1T2	16	3,906259	1,5951383	,3987846
PC07X1T2	16	3,863886	1,7249508	,4312377
PC08X1T2	16	3,800454	1,7097257	,4274314
PC09X1T2	16	3,557368	1,6801392	,4200348
PC10X1T2	16	3,515126	1,6889102	,4222276
PC01X1T3	16	3,307049	1,7991258	,4497815
PC02X1T3	16	3,080507	1,8654633	,4663658
PC03X1T3	16	2,923361	1,9232285	,4808071
PC04X1T3	16	2,775906	1,8204132	,4551033
PC05X1T3	16	2,670548	1,6878743	,4219686
PC06X1T3	16	2,563398	1,6597106	,4149277
PC07X1T3	16	2,331343	1,5299921	,3824980
PC08X1T3	16	2,435386	1,2967245	,3241811
PC09X1T3	16	2,668094	1,1048266	,2762067
PC10X1T3	16	4,707915	1,9280190	,4820047
PC01X2T1	16	4,443030	1,8252421	,4563105
PC02X2T1	16	3,495599	1,4669316	,3667329
PC03X2T1	16	3,144435	1,3647787	,3411947
PC04X2T1	16	2,806316	1,2643298	,3160824
PC05X2T1	16	2,658256	1,1902732	,2975683
PC06X2T1	16	2,654546	1,0879805	,2719951
PC07X2T1	16	2,843981	1,0272846	,2568211
PC08X2T1	16	2,977042	,9603266	,2400816
PC09X2T1	16	3,027269	1,0199636	,2549909
PC10X2T1	16	3,057249	1,0859836	,2714959
PC01X2T2	16	3,042065	1,1895070	,2973767
PC02X2T2	16	3,040993	1,2887121	,3221780
PC03X2T2	16	2,932513	1,2847087	,3211772
PC04X2T2	16	2,865668	1,3723544	,3430886

One-Sample Statistics

	N	Mean	Std. Deviation	Std. Error Mean
PC05X2T2	16	2,784789	1,4740973	,3685243
PC06X2T2	16	2,629589	1,3826382	,3456596
PC07X2T2	16	2,473439	1,4121264	,3530316
PC08X2T2	16	2,314565	1,2886610	,3221653
PC09X2T2	16	2,415523	1,4304229	,3576057
PC10X2T2	16	2,347188	1,4829528	,3707382
PC01X2T3	16	2,307948	1,5403511	,3850878
PC02X2T3	16	2,207470	1,6005380	,4001345
PC03X2T3	16	2,136508	1,4491573	,3622893
PC04X2T3	16	2,082487	1,3984973	,3496243
PC05X2T3	16	2,073812	1,3612703	,3403176
PC06X2T3	16	2,040964	1,4156468	,3539117
PC07X2T3	16	2,306634	1,5969359	,3992340
PC08X2T3	16	2,241906	1,8937325	,4734331
PC09X2T3	16	2,900357	2,2893941	,5723485
PC10X2T3	16	4,734107	4,0178465	1,0044616
PC01X3T1	16	3,322506	1,3619903	,3404976
PC02X3T1	16	2,528306	1,0777655	,2694414
PC03X3T1	16	2,365751	,9160564	,2290141
PC04X3T1	16	2,407253	,8249307	,2062327
PC05X3T1	16	2,379726	,7771101	,1942775
PC06X3T1	16	2,363699	,7883418	,1970855
PC07X3T1	16	2,479910	,9352831	,2338208
PC08X3T1	16	2,489736	,9896437	,2474109
PC09X3T1	16	2,539704	1,0222465	,2555616
PC10X3T1	16	2,680054	1,0314112	,2578528
PC01X3T2	16	2,706153	1,0987040	,2746760
PC02X3T2	16	2,520384	1,0420537	,2605134
PC03X3T2	16	2,514130	1,1529330	,2882333
PC04X3T2	16	2,406894	1,1421329	,2855332
PC05X3T2	16	2,306631	1,1006371	,2751593
PC06X3T2	16	2,263676	1,0696133	,2674033
PC07X3T2	16	2,143115	1,1450463	,2862616
PC08X3T2	16	2,050831	1,0705076	,2676269
PC09X3T2	16	2,120636	1,0231930	,2557982
PC10X3T2	16	1,947274	1,0193580	,2548395
PC01X3T3	16	1,983883	1,0891894	,2722974
PC02X3T3	16	1,962474	1,1319546	,2829887
PC03X3T3	16	1,982679	1,0957576	,2739394
PC04X3T3	16	2,025269	1,2619872	,3154968
PC05X3T3	16	2,023726	1,2652678	,3163169
PC06X3T3	16	2,218909	1,4342058	,3585515
PC07X3T3	16	2,409717	1,4872943	,3718236
PC08X3T3	16	2,590641	1,5177616	,3794404

One-Sample Statistics

	N	Mean	Std. Deviation	Std. Error Mean
PC09X3T3	16	3,167480	2,1376788	,5344197
PC10X3T3	16	5,215004	4,2698381	1,0674595

One-Sample Test

	Test Value = 0					
					95% Confidence Interval of the Difference	
	t	df	Sig. (2-tailed)	Mean Difference	Lower	Upper
PC01X1T1	14,149	15	,000	8,3016949	7,051066	9,552324
PC02X1T1	13,991	15	,000	6,6842695	5,665990	7,702549
PC03X1T1	13,505	15	,000	5,9117536	4,978745	6,844763
PC04X1T1	11,533	15	,000	5,4270806	4,424112	6,430049
PC05X1T1	10,648	15	,000	5,0280646	4,021535	6,034594
PC06X1T1	10,283	15	,000	4,8981130	3,882847	5,913379
PC07X1T1	10,738	15	,000	4,7644015	3,818677	5,710126
PC08X1T1	11,276	15	,000	4,5848854	3,718264	5,451507
PC09X1T1	11,775	15	,000	4,4873373	3,675039	5,299636
PC10X1T1	11,906	15	,000	4,2908630	3,522717	5,059009
PC01X1T2	11,784	15	,000	4,2361120	3,469889	5,002335
PC02X1T2	11,759	15	,000	4,1809009	3,423058	4,938744
PC03X1T2	10,339	15	,000	4,0469528	3,212615	4,881291
PC04X1T2	10,186	15	,000	4,0437574	3,197568	4,889947
PC05X1T2	10,411	15	,000	4,0581897	3,227372	4,889007
PC06X1T2	9,795	15	,000	3,9062595	3,056270	4,756249
PC07X1T2	8,960	15	,000	3,8638855	2,944724	4,783047
PC08X1T2	8,891	15	,000	3,8004536	2,889405	4,711502
PC09X1T2	8,469	15	,000	3,5573676	2,662085	4,452651
PC10X1T2	8,325	15	,000	3,5151260	2,615169	4,415083
PC01X1T3	7,353	15	,000	3,3070491	2,348363	4,265736
PC02X1T3	6,605	15	,000	3,0805072	2,086472	4,074542
PC03X1T3	6,080	15	,000	2,9233609	1,898545	3,948177
PC04X1T3	6,100	15	,000	2,7759061	1,805876	3,745936
PC05X1T3	6,329	15	,000	2,6705475	1,771143	3,569952
PC06X1T3	6,178	15	,000	2,5633978	1,679000	3,447795
PC07X1T3	6,095	15	,000	2,3313433	1,516068	3,146619
PC08X1T3	7,512	15	,000	2,4353863	1,744411	3,126362
PC09X1T3	9,660	15	,000	2,6680940	2,079373	3,256815
PC10X1T3	9,767	15	,000	4,7079151	3,680546	5,735284
PC01X2T1	9,737	15	,000	4,4430295	3,470427	5,415632
PC02X2T1	9,532	15	,000	3,4955987	2,713926	4,277271
PC03X2T1	9,216	15	,000	3,1444349	2,417196	3,871674
PC04X2T1	8,878	15	,000	2,8063164	2,132603	3,480030
PC05X2T1	8,933	15	,000	2,6582555	2,024004	3,292507
PC06X2T1	9,760	15	,000	2,6545459	2,074802	3,234290

One-Sample Test

	Test Value = 0					
					95% Confidence Interval of the Difference	
	t	df	Sig. (2-tailed)	Mean Difference	Lower	Upper
PC07X2T1	11,074	15	,000	2,8439808	2,296579	3,391382
PC08X2T1	12,400	15	,000	2,9770422	2,465320	3,488764
PC09X2T1	11,872	15	,000	3,0272688	2,483769	3,570769
PC10X2T1	11,261	15	,000	3,0572495	2,478570	3,635929
PC01X2T2	10,230	15	,000	3,0420648	2,408221	3,675908
PC02X2T2	9,439	15	,000	3,0409935	2,354287	3,727700
PC03X2T2	9,131	15	,000	2,9325132	2,247940	3,617086
PC04X2T2	8,353	15	,000	2,8656679	2,134392	3,596944
PC05X2T2	7,557	15	,000	2,7847887	1,999298	3,570280
PC06X2T2	7,607	15	,000	2,6295887	1,892833	3,366345
PC07X2T2	7,006	15	,000	2,4734392	1,720970	3,225908
PC08X2T2	7,184	15	,000	2,3145649	1,627886	3,001244
PC09X2T2	6,755	15	,000	2,4155233	1,653305	3,177742
PC10X2T2	6,331	15	,000	2,3471882	1,556978	3,137398
PC01X2T3	5,993	15	,000	2,3079475	1,487152	3,128743
PC02X2T3	5,517	15	,000	2,2074701	1,354604	3,060337
PC03X2T3	5,897	15	,000	2,1365080	1,364307	2,908709
PC04X2T3	5,956	15	,000	2,0824865	1,337280	2,827693
PC05X2T3	6,094	15	,000	2,0738117	1,348442	2,799181
PC06X2T3	5,767	15	,000	2,0409643	1,286619	2,795309
PC07X2T3	5,778	15	,000	2,3066345	1,455687	3,157582
PC08X2T3	4,735	15	,000	2,2419059	1,232807	3,251005
PC09X2T3	5,067	15	,000	2,9003572	1,680425	4,120289
PC10X2T3	4,713	15	,000	4,7341068	2,593148	6,875066
PC01X3T1	9,758	15	,000	3,3225058	2,596752	4,048259
PC02X3T1	9,384	15	,000	2,5283059	1,954005	3,102607
PC03X3T1	10,330	15	,000	2,3657509	1,877619	2,853883
PC04X3T1	11,673	15	,000	2,4072529	1,967678	2,846827
PC05X3T1	12,249	15	,000	2,3797261	1,965633	2,793819
PC06X3T1	11,993	15	,000	2,3636992	1,943621	2,783777
PC07X3T1	10,606	15	,000	2,4799099	1,981533	2,978287
PC08X3T1	10,063	15	,000	2,4897362	1,962392	3,017080
PC09X3T1	9,938	15	,000	2,5397038	1,994987	3,084421
PC10X3T1	10,394	15	,000	2,6800544	2,130454	3,229655
PC01X3T2	9,852	15	,000	2,7061526	2,120695	3,291611
PC02X3T2	9,675	15	,000	2,5203844	1,965113	3,075656
PC03X3T2	8,723	15	,000	2,5141299	1,899775	3,128484
PC04X3T2	8,429	15	,000	2,4068936	1,798294	3,015493
PC05X3T2	8,383	15	,000	2,3066306	1,720142	2,893119
PC06X3T2	8,465	15	,000	2,2636765	1,693720	2,833633
PC07X3T2	7,487	15	,000	2,1431153	1,532963	2,753267

One-Sample Test

	Test Value = 0					
					95% Confidence Interval of the Difference	
	t	df	Sig. (2-tailed)	Mean Difference	Lower	Upper
PC08X3T2	7,663	15	,000	2,0508313	1,480398	2,621265
PC09X3T2	8,290	15	,000	2,1206360	1,575415	2,665857
PC10X3T2	7,641	15	,000	1,9472735	1,404096	2,490451
PC01X3T3	7,286	15	,000	1,9838826	1,403495	2,564271
PC02X3T3	6,935	15	,000	1,9624738	1,359298	2,565650
PC03X3T3	7,238	15	,000	1,9826792	1,398791	2,566567
PC04X3T3	6,419	15	,000	2,0252693	1,352804	2,697735
PC05X3T3	6,398	15	,000	2,0237264	1,349513	2,697940
PC06X3T3	6,189	15	,000	2,2189088	1,454674	2,983143
PC07X3T3	6,481	15	,000	2,4097170	1,617194	3,202240
PC08X3T3	6,828	15	,000	2,5906406	1,781883	3,399399
PC09X3T3	5,927	15	,000	3,1674798	2,028391	4,306568
PC10X3T3	4,885	15	,000	5,2150036	2,939767	7,490240

C.3 ANÁLISE ESTATÍSTICA DA VARIAÇÃO DE ÁREAS DOS CANAIS E RAÍZES

```
*GET
  FILE='C:\Users\WAGNER01\Consultorias\Cons2010\CarolineMarca\ARQ-CM-TRACAD
O-V02.sav'.
*DATASET NAME DataSet1 WINDOW=FRONT.

*SAVE TRANSLATE OUTFILE=
    'C:\Users\WAGNER01\Consultorias\Cons2010\CarolineMarca\ARQ-CM-TRACADO-V
03.xlsx'
  /TYPE=XLS
  /VERSION=12
  /MAP
  /REPLACE
  /FIELDNAMES
  /CELLS=VALUES.

************************.

*GET DATA /TYPE=XLSX
  /FILE='C:\Users\WAGNER01\Consultorias\Cons2010\CarolineMarca\ARQ-CM-TRACA
DO-V04.xlsx'
  /SHEET=name 'Sheet1'
  /CELLRANGE=range 'A1:NW20'
  /READNAMES=on
  /ASSUMEDSTRWIDTH=32767.
*DATASET NAME DataSet1 WINDOW=FRONT.

GET DATA /TYPE=XLSX
  /FILE=
    'C:\Users\Mario\Documents\DocsMario\A01-Cons\MWC\Cons2010\CarolineMarca
\ARQ-CM-TRACADO-V04.xlsx'
  /SHEET=name 'Sheet1'
  /CELLRANGE=range 'A1:NW20'
  /READNAMES=on
  /ASSUMEDSTRWIDTH=32767.
DATASET NAME DataSet2 WINDOW=FRONT.


DATASET ACTIVATE DataSet1.
```

Dataset Activate

Warnings

Unknown dataset DataSet1. Execution of this command stops.

```
RECODE C01S1T1 C02S1T1 C03S1T1 C04S1T1 C05S1T1 C06S1T1 C07S1T1 C08S1T1 C09S
1T1
    C10S1T1 C01S1T2 C02S1T2 C03S1T2 C04S1T2 C05S1T2 C06S1T2 C07S1T2 C08S1T2
 C09S1T2 C10S1T2
    C01S1T3 C02S1T3 C03S1T3 C04S1T3 C05S1T3 C06S1T3 C07S1T3 C08S1T3 C09S1T3
 C10S1T3 C01S2T1 C02S2T1
    C03S2T1 C04S2T1 C05S2T1 C06S2T1 C07S2T1 C08S2T1 C09S2T1 C10S2T1 C01S2T2
 C02S2T2 C03S2T2 C04S2T2
    C05S2T2 C06S2T2 C07S2T2 C08S2T2 C09S2T2 C10S2T2 C01S2T3 C02S2T3 C03S2T3
 C04S2T3 C05S2T3 C06S2T3
    C07S2T3 C08S2T3 C09S2T3 C10S2T3 C01S3T1 C02S3T1 C03S3T1 C04S3T1 C05S3T1
 C06S3T1 C07S3T1
    C08S3T1 C09S3T1 C10S3T1 C01S3T2 C02S3T2 C03S3T2 C04S3T2 C05S3T2 C06S3T2
 C07S3T2 C08S3T2 C09S3T2
    C10S3T2 C01S3T3 C02S3T3 C03S3T3 C04S3T3 C05S3T3 C06S3T3 C07S3T3 C08S3T3
 C09S3T3 C10S3T3 (0=SYSMIS).

FREQUENCIES VARIABLES=C01S1T1 C02S1T1 C03S1T1 C04S1T1 C05S1T1 C06S1T1 C07S1
T1 C08S1T1 C09S1T1
    C10S1T1 C01S1T2 C02S1T2 C03S1T2 C04S1T2 C05S1T2 C06S1T2 C07S1T2 C08S1T2
 C09S1T2 C10S1T2
    C01S1T3 C02S1T3 C03S1T3 C04S1T3 C05S1T3 C06S1T3 C07S1T3 C08S1T3 C09S1T3
 C10S1T3 C01S2T1 C02S2T1
    C03S2T1 C04S2T1 C05S2T1 C06S2T1 C07S2T1 C08S2T1 C09S2T1 C10S2T1 C01S2T2
 C02S2T2 C03S2T2 C04S2T2
    C05S2T2 C06S2T2 C07S2T2 C08S2T2 C09S2T2 C10S2T2 C01S2T3 C02S2T3 C03S2T3
 C04S2T3 C05S2T3 C06S2T3
    C07S2T3 C08S2T3 C09S2T3 C10S2T3 C01S3T1 C02S3T1 C03S3T1 C04S3T1 C05S3T1
 C06S3T1 C07S3T1
    C08S3T1 C09S3T1 C10S3T1 C01S3T2 C02S3T2 C03S3T2 C04S3T2 C05S3T2 C06S3T2
 C07S3T2 C08S3T2 C09S3T2
    C10S3T2 C01S3T3 C02S3T3 C03S3T3 C04S3T3 C05S3T3 C06S3T3 C07S3T3 C08S3T3
 C09S3T3 C10S3T3
  /STATISTICS=STDDEV MINIMUM MAXIMUM MEAN MEDIAN
  /ORDER=ANALYSIS/format=notable.
```

Frequencies

[DataSet2]

Statistics

		C01S1T1	C02S1T1	C03S1T1	C04S1T1	C05S1T1
N	Valid	16	16	16	16	16
	Missing	3	3	3	3	3
Mean		17,005446	16,528393	15,945907	15,314131	14,809452
Median		15,901212	15,338847	14,977827	14,315106	13,974915
Std. Deviation		4,0276039	3,6084242	3,2461312	3,1160742	3,1235197
Minimum		12,5107	12,3580	12,3931	12,0341	11,8078
Maximum		26,3750	24,7057	23,1764	22,3027	22,9232

Statistics

		C06S1T1	C07S1T1	C08S1T1	C09S1T1	C10S1T1
N	Valid	16	16	16	16	16
	Missing	3	3	3	3	3
Mean		14,175847	13,565417	12,937577	12,465892	11,880040
Median		13,621741	13,361164	13,061736	12,839942	12,180048
Std. Deviation		2,8022167	2,6106566	2,4422770	2,4841879	2,5060386
Minimum		10,4537	9,6775	9,2409	8,7071	8,4001
Maximum		20,8019	19,4903	18,7667	18,5030	17,6463

Statistics

		C01S1T2	C02S1T2	C03S1T2	C04S1T2	C05S1T2
N	Valid	16	16	16	16	16
	Missing	3	3	3	3	3
Mean		11,632635	11,248811	10,789210	10,495215	10,102727
Median		11,665819	11,156944	10,485511	10,361749	9,840996
Std. Deviation		2,3726539	2,2108534	2,1825065	2,2378536	2,2360806
Minimum		8,0147	7,7732	7,5095	7,2506	6,8015
Maximum		16,9941	15,9587	15,3473	14,9757	14,1058

Statistics

		C06S1T2	C07S1T2	C08S1T2	C09S1T2	C10S1T2
N	Valid	16	16	16	16	16
	Missing	3	3	3	3	3
Mean		9,818885	9,435024	9,057416	8,679743	8,233494
Median		9,568890	9,124272	8,732675	8,338554	7,985612
Std. Deviation		2,2722277	2,3088649	2,3197947	2,3638767	2,2944911
Minimum		6,3410	6,0790	5,8046	5,5045	5,0974
Maximum		13,2937	12,7041	12,3680	11,7779	11,3378

Statistics

		C01S1T3	C02S1T3	C03S1T3	C04S1T3	C05S1T3
N	Valid	16	16	16	16	16
	Missing	3	3	3	3	3
Mean		7,769272	7,288735	6,772154	6,228501	5,547722
Median		7,628975	7,155267	6,570774	6,129586	5,556586
Std. Deviation		2,2452852	2,1715847	2,1299993	1,9719393	1,7434287
Minimum		4,7353	4,3850	3,9883	3,6422	3,0525
Maximum		10,9527	10,3297	9,4577	8,9170	8,3793

Statistics

		C06S1T3	C07S1T3	C08S1T3	C09S1T3	C10S1T3
N	Valid	16	16	16	16	16
	Missing	3	3	3	3	3
Mean		4,845588	4,107845	3,380264	2,611085	1,601637
Median		4,922227	4,181205	3,351078	2,562576	1,382534
Std. Deviation		1,5691432	1,3651515	1,1454297	,9501093	,7666739
Minimum		2,4234	1,9395	1,5059	1,2076	,5069
Maximum		7,5186	6,5925	5,5141	4,3694	3,5521

Statistics

		C01S2T1	C02S2T1	C03S2T1	C04S2T1	C05S2T1
N	Valid	16	16	16	16	16
	Missing	3	3	3	3	3
Mean		9,432318	9,023188	8,653111	8,297370	8,102223
Median		9,286194	8,722512	8,547340	8,286313	7,828431
Std. Deviation		2,6797384	2,4558830	1,9501917	1,8452077	1,8326324
Minimum		5,8523	5,6468	5,5562	5,4595	5,4326
Maximum		16,8011	14,9302	12,7500	12,1959	11,4384

Statistics

		C06S2T1	C07S2T1	C08S2T1	C09S2T1	C10S2T1
N	Valid	16	16	16	16	16
	Missing	3	3	3	3	3
Mean		7,819407	7,518976	7,242963	6,896787	6,691776
Median		7,621387	7,199494	6,964917	6,585950	6,663565
Std. Deviation		1,7734868	1,7599551	1,6797632	1,6025239	1,5782104
Minimum		5,3723	5,2119	5,0666	4,8901	4,6282
Maximum		10,9285	10,6583	10,2408	9,8419	9,2760

Statistics

		C01S2T2	C02S2T2	C03S2T2	C04S2T2	C05S2T2
N	Valid	16	16	16	16	16
	Missing	3	3	3	3	3
Mean		6,372944	6,133055	5,914846	5,658995	5,491002
Median		6,375004	6,061078	5,919724	5,497615	5,352575
Std. Deviation		1,4533562	1,3658792	1,2916556	1,2793004	1,2924728
Minimum		4,3746	4,1214	3,9523	3,7155	3,4077
Maximum		8,8550	8,4465	8,0437	7,7324	7,5681

Statistics

		C06S2T2	C07S2T2	C08S2T2	C09S2T2	C10S2T2
N	Valid	16	16	16	16	16
	Missing	3	3	3	3	3
Mean		5,271519	5,061467	4,857404	4,639845	4,388737
Median		5,130355	4,825534	4,673558	4,460443	4,160392
Std. Deviation		1,2636779	1,2344238	1,2069512	1,1713383	1,1379931
Minimum		3,1917	3,0751	2,9784	2,6901	2,3440
Maximum		7,2962	7,0508	6,7290	6,4012	6,0821

Statistics

		C01S2T3	C02S2T3	C03S2T3	C04S2T3	C05S2T3
N	Valid	16	16	16	16	16
	Missing	3	3	3	3	3
Mean		4,147899	3,907657	3,630289	3,369831	3,054035
Median		3,936654	3,600398	3,325064	3,082462	2,845717
Std. Deviation		1,0920822	1,1020106	1,0914456	1,0960343	1,0453133
Minimum		1,9941	1,7539	1,5575	1,3507	1,2414
Maximum		5,6685	5,7560	5,7348	5,6138	5,5245

Statistics

		C06S2T3	C07S2T3	C08S2T3	C09S2T3	C10S2T3	C01S3T1
N	Valid	16	16	16	16	16	16
	Missing	3	3	3	3	3	3
Mean		2,711192	2,345424	1,955915	1,558304	1,110314	7,940788
Median		2,554337	2,280302	1,815917	1,358686	,849422	7,671250
Std. Deviation		,9882715	,9233843	,8295978	,7363525	,6857298	2,1545532
Minimum		1,0866	,8763	,7584	,5845	,2953	4,4053
Maximum		4,9851	4,4973	3,8590	3,2698	2,4212	13,4659

Statistics

		C02S3T1	C03S3T1	C04S3T1	C05S3T1	C06S3T1
N	Valid	16	16	16	16	16
	Missing	3	3	3	3	3
Mean		7,805081	7,487700	7,194881	6,925619	6,653506
Median		7,612900	7,163700	6,847200	6,651850	6,509600
Std. Deviation		2,1714167	2,0353975	1,9446564	1,7737827	1,7613593
Minimum		4,2705	4,1751	3,9891	3,9272	3,6643
Maximum		12,8966	12,0454	11,7653	11,1738	10,9245

Statistics

		C07S3T1	C08S3T1	C09S3T1	C10S3T1	C01S3T2
N	Valid	16	16	16	16	16
	Missing	3	3	3	3	3
Mean		6,462438	6,309481	6,125069	5,891988	5,669781
Median		6,239750	6,012050	5,663450	5,524300	5,290550
Std. Deviation		1,6883380	1,7407106	1,6482198	1,6191463	1,6290583
Minimum		3,6280	3,4965	3,6089	3,5620	3,3955
Maximum		10,3843	10,0656	9,5687	8,9785	8,6595

Statistics

		C02S3T2	C03S3T2	C04S3T2	C05S3T2	C06S3T2
N	Valid	16	16	16	16	16
	Missing	3	3	3	3	3
Mean		5,489562	5,257731	5,037038	4,909463	4,681306
Median		5,173950	5,130350	4,932850	4,715150	4,565350
Std. Deviation		1,6163702	1,5122625	1,4786721	1,4167645	1,3756670
Minimum		3,1783	3,1354	2,9875	2,9463	2,7520
Maximum		8,3338	7,8430	7,5043	7,4575	7,0798

Statistics

		C07S3T2	C08S3T2	C09S3T2	C10S3T2	C01S3T3
N	Valid	16	16	16	16	16
	Missing	3	3	3	3	3
Mean		4,449300	4,238325	4,028706	3,836644	3,612404
Median		4,304150	4,051950	3,827150	3,638550	3,372328
Std. Deviation		1,3345697	1,3327034	1,2758402	1,2532471	1,2043191
Minimum		2,6150	2,4984	2,3514	2,1733	1,9820
Maximum		6,7208	6,4993	6,1320	5,9004	5,7001

Statistics

		C02S3T3	C03S3T3	C04S3T3	C05S3T3	C06S3T3
N	Valid	16	16	16	16	16
	Missing	3	3	3	3	3
Mean		3,334551	3,082894	2,841838	2,565763	2,297894
Median		3,135801	2,894500	2,604000	2,330150	2,041000
Std. Deviation		1,1669998	1,1375779	1,0973147	1,0353160	,9592563
Minimum		1,8151	1,5752	1,3910	1,2041	1,0576
Maximum		5,5002	5,2609	4,9803	4,7293	4,2871

Statistics

		C07S3T3	C08S3T3	C09S3T3	C10S3T3
N	Valid	16	16	16	16
	Missing	3	3	3	3
Mean		2,038156	1,721069	1,394587	1,018806
Median		1,791400	1,550100	1,276500	,883700
Std. Deviation		,8858662	,8036019	,7271810	,7018353
Minimum		,9136	,7176	,5819	,2783
Maximum		3,8825	3,3682	3,0170	2,5379

```
T-TEST
  /TESTVAL=0
  /MISSING=ANALYSIS
  /VARIABLES=C01S1T1 C02S1T1 C03S1T1 C04S1T1 C05S1T1 C06S1T1 C07S1T1 C08S1T
1 C09S1T1
    C10S1T1 C01S1T2 C02S1T2 C03S1T2 C04S1T2 C05S1T2 C06S1T2 C07S1T2 C08S1T2
 C09S1T2 C10S1T2
    C01S1T3 C02S1T3 C03S1T3 C04S1T3 C05S1T3 C06S1T3 C07S1T3 C08S1T3 C09S1T3
 C10S1T3 C01S2T1 C02S2T1
    C03S2T1 C04S2T1 C05S2T1 C06S2T1 C07S2T1 C08S2T1 C09S2T1 C10S2T1 C01S2T2
 C02S2T2 C03S2T2 C04S2T2
    C05S2T2 C06S2T2 C07S2T2 C08S2T2 C09S2T2 C10S2T2 C01S2T3 C02S2T3 C03S2T3
 C04S2T3 C05S2T3 C06S2T3
    C07S2T3 C08S2T3 C09S2T3 C10S2T3 C01S3T1 C02S3T1 C03S3T1 C04S3T1 C05S3T1
 C06S3T1 C07S3T1
    C08S3T1 C09S3T1 C10S3T1 C01S3T2 C02S3T2 C03S3T2 C04S3T2 C05S3T2 C06S3T2
 C07S3T2 C08S3T2 C09S3T2
    C10S3T2 C01S3T3 C02S3T3 C03S3T3 C04S3T3 C05S3T3 C06S3T3 C07S3T3 C08S3T3
 C09S3T3 C10S3T3
  /CRITERIA=CI(.95).
```

T-Test

[DataSet2]

One-Sample Statistics

	N	Mean	Std. Deviation	Std. Error Mean
C01S1T1	16	17,005446	4,0276039	1,0069010
C02S1T1	16	16,528393	3,6084242	,9021060
C03S1T1	16	15,945907	3,2461312	,8115328
C04S1T1	16	15,314131	3,1160742	,7790186
C05S1T1	16	14,809452	3,1235197	,7808799
C06S1T1	16	14,175847	2,8022167	,7005542
C07S1T1	16	13,565417	2,6106566	,6526642
C08S1T1	16	12,937577	2,4422770	,6105692
C09S1T1	16	12,465892	2,4841879	,6210470
C10S1T1	16	11,880040	2,5060386	,6265096
C01S1T2	16	11,632635	2,3726539	,5931635
C02S1T2	16	11,248811	2,2108534	,5527134
C03S1T2	16	10,789210	2,1825065	,5456266
C04S1T2	16	10,495215	2,2378536	,5594634
C05S1T2	16	10,102727	2,2360806	,5590202
C06S1T2	16	9,818885	2,2722277	,5680569
C07S1T2	16	9,435024	2,3088649	,5772162
C08S1T2	16	9,057416	2,3197947	,5799487
C09S1T2	16	8,679743	2,3638767	,5909692
C10S1T2	16	8,233494	2,2944911	,5736228
C01S1T3	16	7,769272	2,2452852	,5613213
C02S1T3	16	7,288735	2,1715847	,5428962
C03S1T3	16	6,772154	2,1299993	,5324998
C04S1T3	16	6,228501	1,9719393	,4929848
C05S1T3	16	5,547722	1,7434287	,4358572
C06S1T3	16	4,845588	1,5691432	,3922858
C07S1T3	16	4,107845	1,3651515	,3412879
C08S1T3	16	3,380264	1,1454297	,2863574
C09S1T3	16	2,611085	,9501093	,2375273
C10S1T3	16	1,601637	,7666739	,1916685
C01S2T1	16	9,432318	2,6797384	,6699346
C02S2T1	16	9,023188	2,4558830	,6139708
C03S2T1	16	8,653111	1,9501917	,4875479
C04S2T1	16	8,297370	1,8452077	,4613019
C05S2T1	16	8,102223	1,8326324	,4581581
C06S2T1	16	7,819407	1,7734868	,4433717
C07S2T1	16	7,518976	1,7599551	,4399888
C08S2T1	16	7,242963	1,6797632	,4199408
C09S2T1	16	6,896787	1,6025239	,4006310
C10S2T1	16	6,691776	1,5782104	,3945526

One-Sample Statistics

	N	Mean	Std. Deviation	Std. Error Mean
C01S2T2	16	6,372944	1,4533562	,3633390
C02S2T2	16	6,133055	1,3658792	,3414698
C03S2T2	16	5,914846	1,2916556	,3229139
C04S2T2	16	5,658995	1,2793004	,3198251
C05S2T2	16	5,491002	1,2924728	,3231182
C06S2T2	16	5,271519	1,2636779	,3159195
C07S2T2	16	5,061467	1,2344238	,3086059
C08S2T2	16	4,857404	1,2069512	,3017378
C09S2T2	16	4,639845	1,1713383	,2928346
C10S2T2	16	4,388737	1,1379931	,2844983
C01S2T3	16	4,147899	1,0920822	,2730205
C02S2T3	16	3,907657	1,1020106	,2755027
C03S2T3	16	3,630289	1,0914456	,2728614
C04S2T3	16	3,369831	1,0960343	,2740086
C05S2T3	16	3,054035	1,0453133	,2613283
C06S2T3	16	2,711192	,9882715	,2470679
C07S2T3	16	2,345424	,9233843	,2308461
C08S2T3	16	1,955915	,8295978	,2073995
C09S2T3	16	1,558304	,7363525	,1840881
C10S2T3	16	1,110314	,6857298	,1714324
C01S3T1	16	7,940787	2,1545532	,5386383
C02S3T1	16	7,805081	2,1714167	,5428542
C03S3T1	16	7,487700	2,0353975	,5088494
C04S3T1	16	7,194881	1,9446564	,4861641
C05S3T1	16	6,925619	1,7737827	,4434457
C06S3T1	16	6,653506	1,7613593	,4403398
C07S3T1	16	6,462438	1,6883380	,4220845
C08S3T1	16	6,309481	1,7407106	,4351777
C09S3T1	16	6,125069	1,6482198	,4120550
C10S3T1	16	5,891988	1,6191463	,4047866
C01S3T2	16	5,669781	1,6290583	,4072646
C02S3T2	16	5,489562	1,6163702	,4040925
C03S3T2	16	5,257731	1,5122625	,3780656
C04S3T2	16	5,037038	1,4786721	,3696680
C05S3T2	16	4,909463	1,4167645	,3541911
C06S3T2	16	4,681306	1,3756670	,3439167
C07S3T2	16	4,449300	1,3345697	,3336424
C08S3T2	16	4,238325	1,3327034	,3331758
C09S3T2	16	4,028706	1,2758402	,3189601
C10S3T2	16	3,836644	1,2532471	,3133118

One-Sample Statistics

	N	Mean	Std. Deviation	Std. Error Mean
C01S3T3	16	3,612404	1,2043191	,3010798
C02S3T3	16	3,334551	1,1669998	,2917499
C03S3T3	16	3,082894	1,1375779	,2843945
C04S3T3	16	2,841837	1,0973147	,2743287
C05S3T3	16	2,565763	1,0353160	,2588290
C06S3T3	16	2,297894	,9592563	,2398141
C07S3T3	16	2,038156	,8858662	,2214666
C08S3T3	16	1,721069	,8036019	,2009005
C09S3T3	16	1,394587	,7271810	,1817953
C10S3T3	16	1,018806	,7018353	,1754588

One-Sample Test

	Test Value = 0					
					95% Confidence Interval of the Difference	
	t	df	Sig. (2-tailed)	Mean Difference	Lower	Upper
C01S1T1	16,889	15	,000	17,0054456	14,859287	19,151604
C02S1T1	18,322	15	,000	16,5283928	14,605599	18,451186
C03S1T1	19,649	15	,000	15,9459070	14,216166	17,675648
C04S1T1	19,658	15	,000	15,3141310	13,653692	16,974570
C05S1T1	18,965	15	,000	14,8094516	13,145045	16,473858
C06S1T1	20,235	15	,000	14,1758467	12,682651	15,669043
C07S1T1	20,785	15	,000	13,5654168	12,174296	14,956537
C08S1T1	21,189	15	,000	12,9375767	11,636179	14,238974
C09S1T1	20,072	15	,000	12,4658919	11,142162	13,789622
C10S1T1	18,962	15	,000	11,8800404	10,544667	13,215414
C01S1T2	19,611	15	,000	11,6326348	10,368337	12,896933
C02S1T2	20,352	15	,000	11,2488106	10,070730	12,426891
C03S1T2	19,774	15	,000	10,7892103	9,626235	11,952186
C04S1T2	18,759	15	,000	10,4952155	9,302747	11,687683
C05S1T2	18,072	15	,000	10,1027270	8,911204	11,294250
C06S1T2	17,285	15	,000	9,8188849	8,608100	11,029670
C07S1T2	16,346	15	,000	9,4350239	8,204717	10,665331
C08S1T2	15,618	15	,000	9,0574158	7,821284	10,293547
C09S1T2	14,687	15	,000	8,6797433	7,420122	9,939364
C10S1T2	14,353	15	,000	8,2334939	7,010846	9,456142
C01S1T3	13,841	15	,000	7,7692719	6,572844	8,965700
C02S1T3	13,426	15	,000	7,2887347	6,131579	8,445891
C03S1T3	12,718	15	,000	6,7721545	5,637158	7,907151
C04S1T3	12,634	15	,000	6,2285014	5,177729	7,279274

One-Sample Test

	Test Value = 0					
					95% Confidence Interval of the Difference	
	t	df	Sig. (2-tailed)	Mean Difference	Lower	Upper
C05S1T3	12,728	15	,000	5,5477222	4,618715	6,476730
C06S1T3	12,352	15	,000	4,8455884	4,009451	5,681726
C07S1T3	12,036	15	,000	4,1078451	3,380407	4,835283
C08S1T3	11,804	15	,000	3,3802643	2,769908	3,990621
C09S1T3	10,993	15	,000	2,6110850	2,104807	3,117363
C10S1T3	8,356	15	,000	1,6016371	1,193105	2,010169
C01S2T1	14,079	15	,000	9,4323177	8,004386	10,860249
C02S2T1	14,696	15	,000	9,0231883	7,714541	10,331836
C03S2T1	17,748	15	,000	8,6531113	7,613927	9,692295
C04S2T1	17,987	15	,000	8,2973696	7,314128	9,280611
C05S2T1	17,684	15	,000	8,1022225	7,125682	9,078763
C06S2T1	17,636	15	,000	7,8194069	6,874383	8,764431
C07S2T1	17,089	15	,000	7,5189762	6,581162	8,456790
C08S2T1	17,248	15	,000	7,2429628	6,347880	8,138045
C09S2T1	17,215	15	,000	6,8967874	6,042863	7,750712
C10S2T1	16,960	15	,000	6,6917758	5,850807	7,532745
C01S2T2	17,540	15	,000	6,3729444	5,598506	7,147383
C02S2T2	17,961	15	,000	6,1330551	5,405229	6,860881
C03S2T2	18,317	15	,000	5,9148460	5,226571	6,603121
C04S2T2	17,694	15	,000	5,6589949	4,977304	6,340686
C05S2T2	16,994	15	,000	5,4910020	4,802292	6,179712
C06S2T2	16,686	15	,000	5,2715192	4,598153	5,944886
C07S2T2	16,401	15	,000	5,0614670	4,403689	5,719245
C08S2T2	16,098	15	,000	4,8574040	4,214265	5,500543
C09S2T2	15,845	15	,000	4,6398452	4,015683	5,264007
C10S2T2	15,426	15	,000	4,3887366	3,782343	4,995130
C01S2T3	15,193	15	,000	4,1478989	3,565969	4,729828
C02S2T3	14,184	15	,000	3,9076574	3,320437	4,494877
C03S2T3	13,305	15	,000	3,6302888	3,048698	4,211879
C04S2T3	12,298	15	,000	3,3698308	2,785795	3,953866
C05S2T3	11,687	15	,000	3,0540345	2,497026	3,611043
C06S2T3	10,973	15	,000	2,7111923	2,184580	3,237805
C07S2T3	10,160	15	,000	2,3454237	1,853387	2,837460
C08S2T3	9,431	15	,000	1,9559154	1,513854	2,397977
C09S2T3	8,465	15	,000	1,5583042	1,165930	1,950679
C10S2T3	6,477	15	,000	1,1103141	,744915	1,475714
C01S3T1	14,742	15	,000	7,9407875	6,792707	9,088868

One-Sample Test

	Test Value = 0					
					95% Confidence Interval of the Difference	
	t	df	Sig. (2-tailed)	Mean Difference	Lower	Upper
C02S3T1	14,378	15	,000	7,8050813	6,648015	8,962148
C03S3T1	14,715	15	,000	7,4877000	6,403113	8,572287
C04S3T1	14,799	15	,000	7,1948813	6,158647	8,231116
C05S3T1	15,618	15	,000	6,9256187	5,980437	7,870801
C06S3T1	15,110	15	,000	6,6535062	5,714944	7,592068
C07S3T1	15,311	15	,000	6,4624375	5,562786	7,362089
C08S3T1	14,499	15	,000	6,3094813	5,381922	7,237040
C09S3T1	14,865	15	,000	6,1250688	5,246794	7,003343
C10S3T1	14,556	15	,000	5,8919875	5,029205	6,754770
C01S3T2	13,922	15	,000	5,6697813	4,801717	6,537845
C02S3T2	13,585	15	,000	5,4895625	4,628260	6,350865
C03S3T2	13,907	15	,000	5,2577312	4,451903	6,063559
C04S3T2	13,626	15	,000	5,0370375	4,249109	5,824966
C05S3T2	13,861	15	,000	4,9094625	4,154522	5,664403
C06S3T2	13,612	15	,000	4,6813062	3,948265	5,414347
C07S3T2	13,336	15	,000	4,4493000	3,738158	5,160442
C08S3T2	12,721	15	,000	4,2383250	3,528178	4,948472
C09S3T2	12,631	15	,000	4,0287063	3,348859	4,708554
C10S3T2	12,245	15	,000	3,8366438	3,168836	4,504452
C01S3T3	11,998	15	,000	3,6124042	2,970668	4,254141
C02S3T3	11,429	15	,000	3,3345510	2,712701	3,956401
C03S3T3	10,840	15	,000	3,0828938	2,476721	3,689066
C04S3T3	10,359	15	,000	2,8418375	2,257120	3,426555
C05S3T3	9,913	15	,000	2,5657625	2,014082	3,117443
C06S3T3	9,582	15	,000	2,2978938	1,786742	2,809045
C07S3T3	9,203	15	,000	2,0381563	1,566111	2,510201
C08S3T3	8,567	15	,000	1,7210688	1,292860	2,149278
C09S3T3	7,671	15	,000	1,3945875	1,007100	1,782075
C10S3T3	5,807	15	,000	1,0188063	,644825	1,392788

ANEXO D. FIGURAS

Figura 1. Fotografia de PmS Trirradiculado

Figura 2. Fotografia de PmS Trirradiculado com presença de cárie

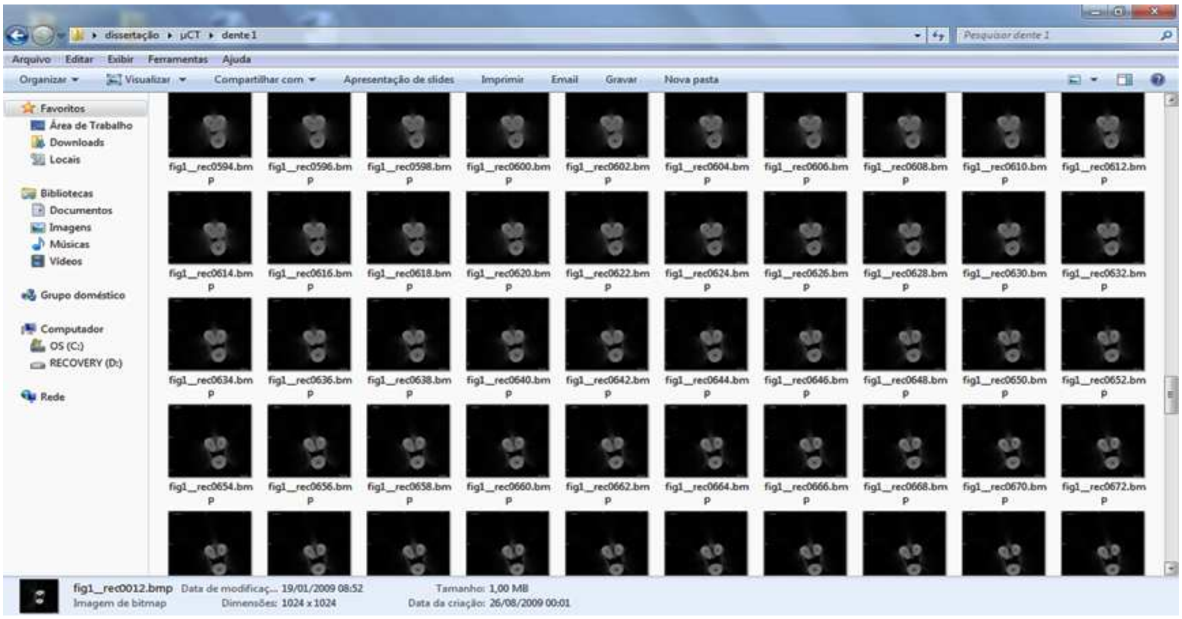

Figura 3. Secções transversais microtomográficas de PmS

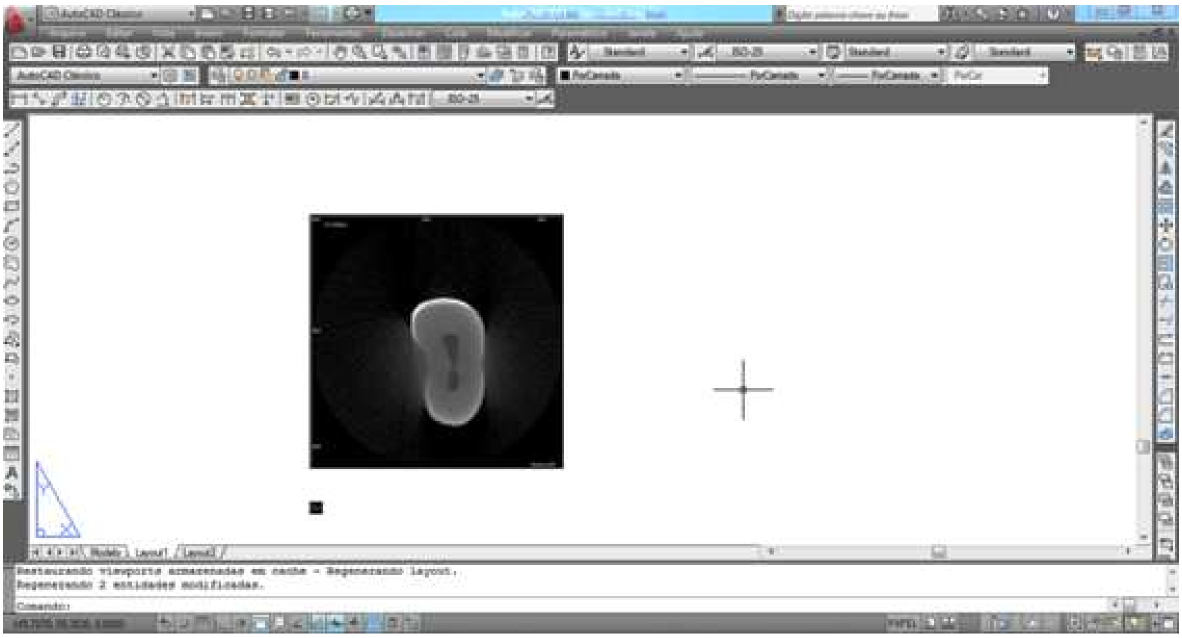

Figura 4. Imagens de µTC e a TCFC de PmS, em formato .bmp na área de trabalho do AutoCAD PmS antes da equivalência de escalas das duas figuras.

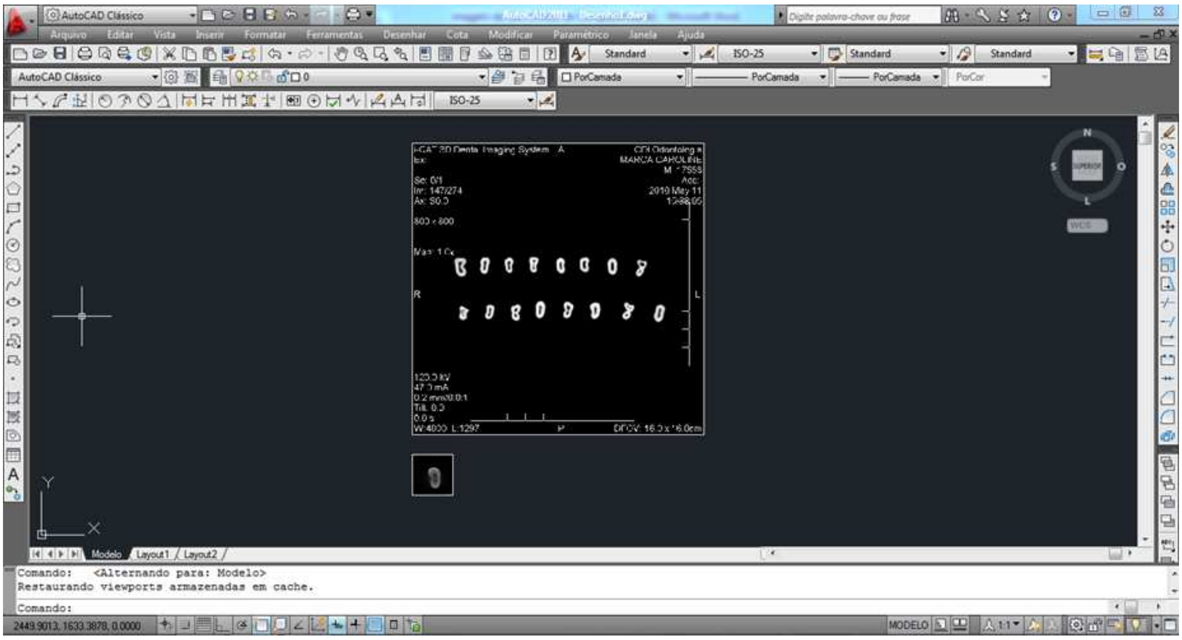

Figura 5. Imagens de µTC e a TCFC de PmS, em formato .bmp na área de trabalho do AutoCAD PmS após equivalência de escalas.

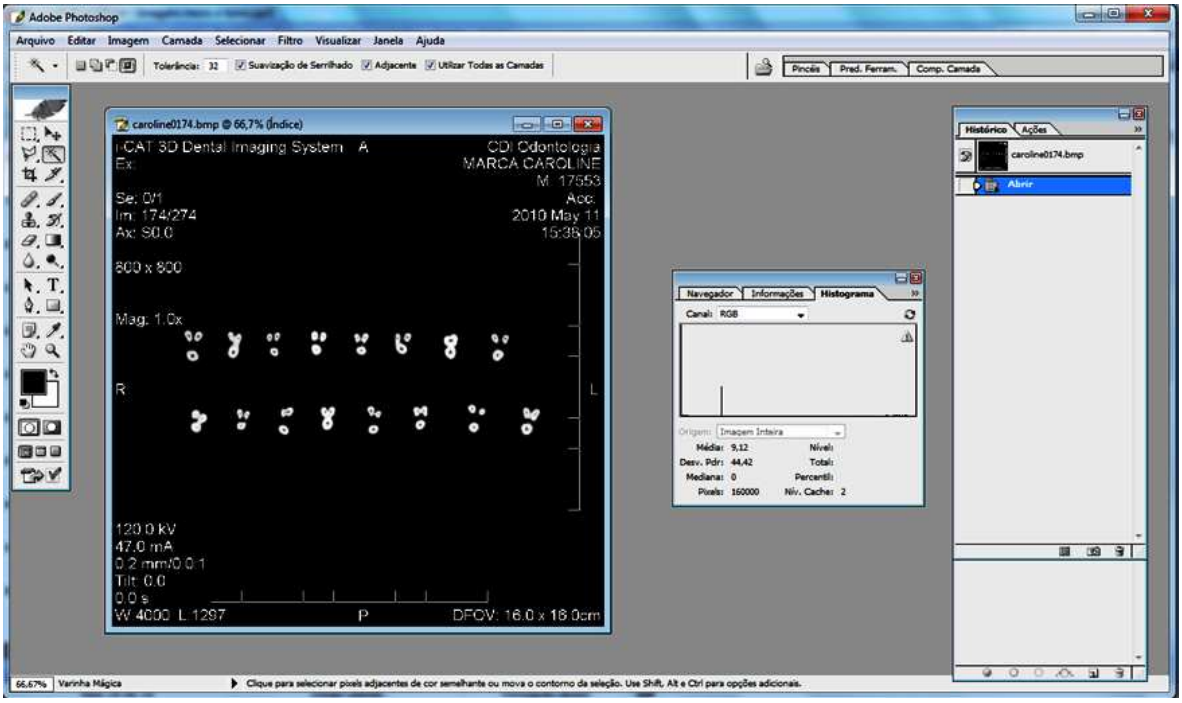

Figura 6. Imagens de TCFC de PmS, na área de trabalho do Photoshop CS

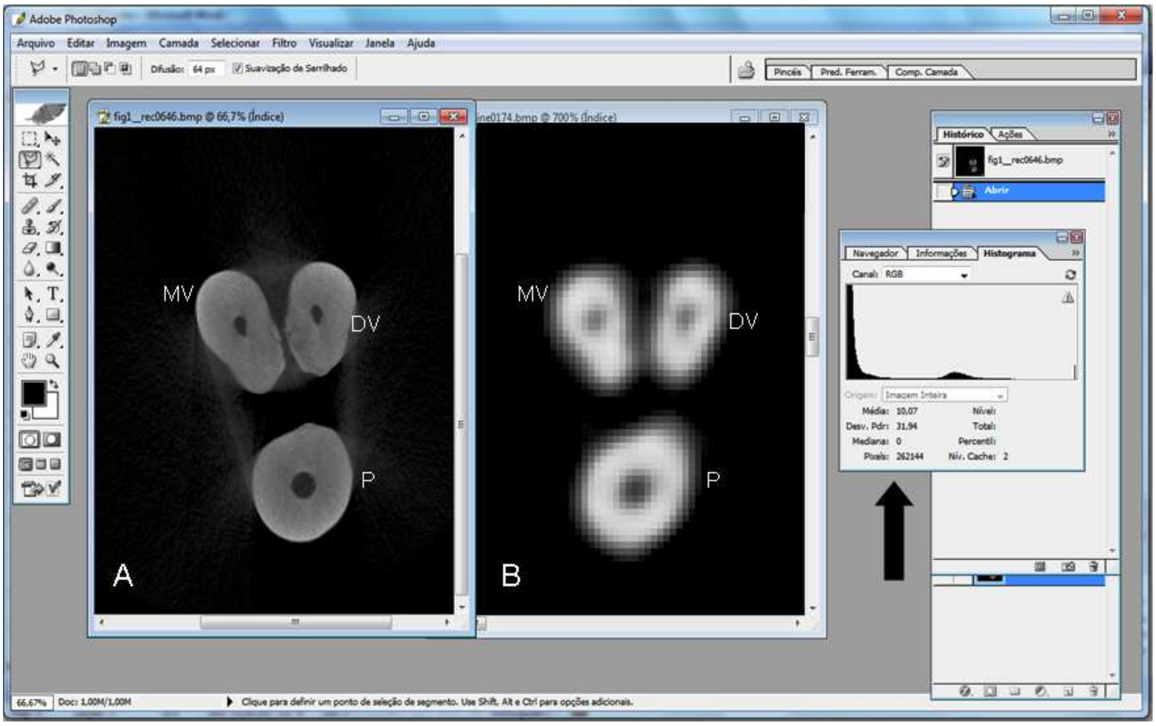

Figura 7. Imagens ampliadas de µTC (A) e a TCFC (B) de PmS, na área de trabalho do Photoshop, com indicação das diferentes raízes (MV=mésio-vestibular, DV=disto-vestibular, P=palatina), e indicação do número de pixels no histograma (seta preta).

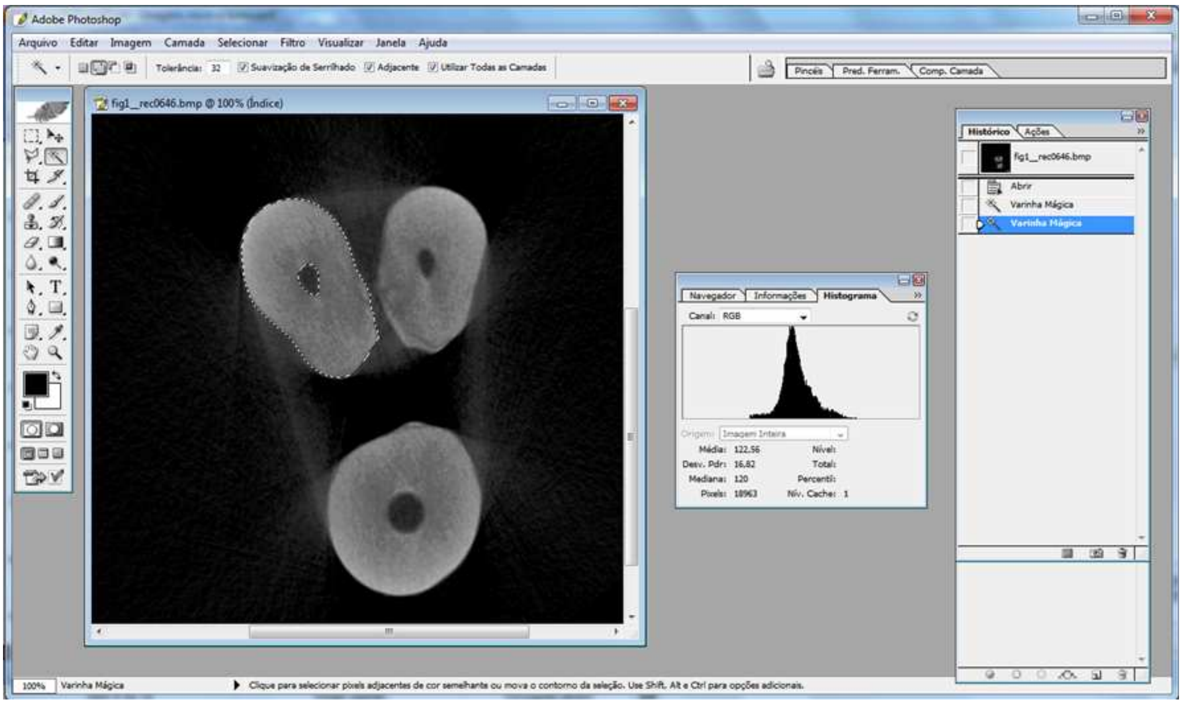

Figura 8. Imagens ampliadas de µTC de PmS, na área de trabalho do Photoshop, com o perímetro da raiz e canal delimitado para posterior mensuração das respectivas áreas.

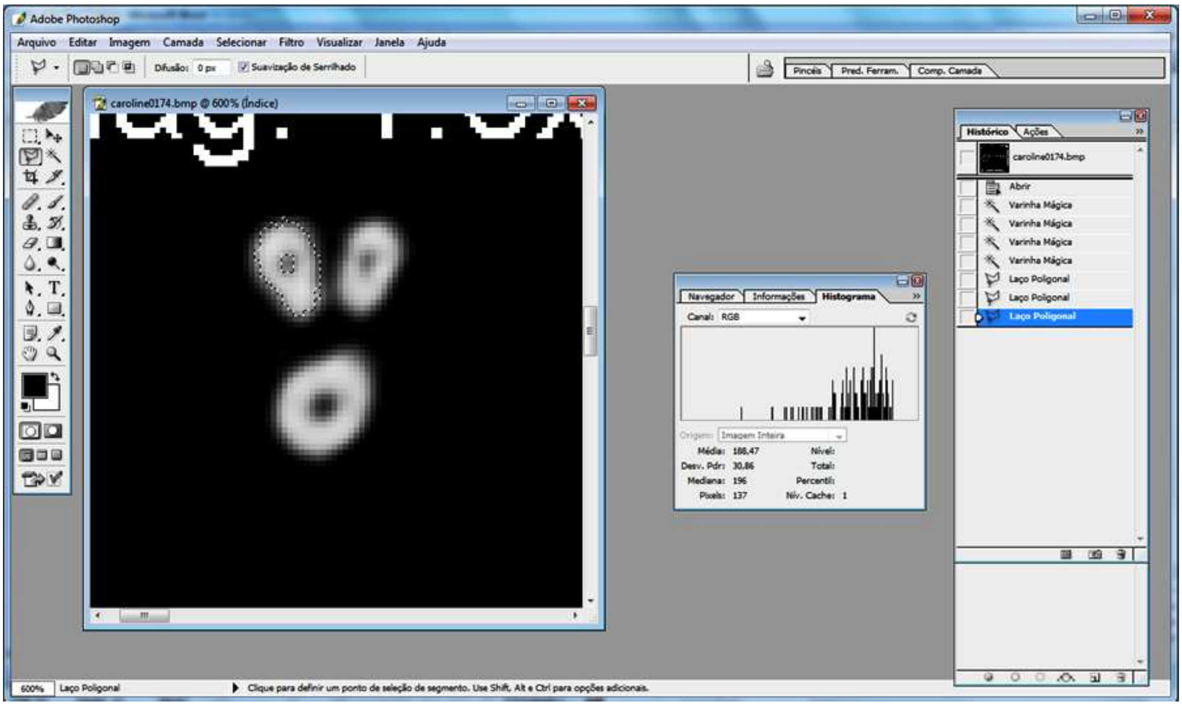

Figura 9. Imagens ampliadas de TCFC de PmS, na área de trabalho do Photoshop, com o perímetro da raiz e canal delimitado para posterior mensuração das respectivas áreas.